DESIGN OF ROAD HUMPS

by

M. V. R. GOPAL

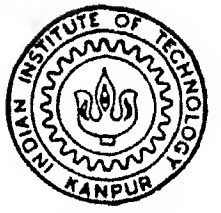

DEPARTMENT OF MECHANICAL ENGINEERING

INDIAN INSTITUTE OF TECHNOLOGY KANPUR

February 1994

DESIGN OF ROAD HUMPS

A Thesis Submitted
in Partial Fulfilment of the Requirements
for the Degree of
MASTER OF TECHNOLOGY

by

M. V. R. Gopal

to the

DEPARTMENT OF MECHANICAL ENGINEERING
INDIAN INSTITUTE OF TECHNOLOGY KANPUR

February, 1991

CERTIFICATE

It is certified that the work contained in this thesis entitled DESIGN OF ROAD HUMPS *by* MANCHELLA VENKATA RATNA GOPAL *has been carried out under our supervision and that this work has not been submitted elsewhere for a degree.*

Dr. AMITABHA MUKHERJEE
Assistant Professor
Dept. of Mechanical Engineering
Indian Institute of Technology
Kanpur-208 016, INDIA

Dr. IGOR. V. LADNIK
Visiting Faculty
Dept. of Mechanical Engineering
Indian Institute of Technology
Kanpur-208 016, INDIA

FEBRUARY, 1994

ABSTRACT

What makes a hump effective? - this is a difficult question. In this analysis we compare humps by modelling passenger comfort and safety along with the rattle space or wheel well clearance. Design considerations for humps involve factors like type of vehicle, allowable speed limit, acceptable discomfort level of passenger etc. A mathematical model representing the vehicle and driver system is developed. The dynamic response of this system is evaluated through computer simulation both in time and frequency domains for a class of humps. It was found that the dynamic effect of humps vary considerably with the type of the vehicle. Size of the hump also plays a major role on its dynamic effects. Simulation results show that humps cannot be designed that will have little or no effect at slow speeds, and the difference in the effects at low and high speeds is not very much. This indicates that humps are poor means of controlling speed, and that other mechanisms should be sought for this purpose.

This small piece of work

is dedicated

to

my beloved parents

sisters and brother

A C K N O W L E D G E M E N T

It gives me immense pleasure to express my sincere thanks to Dr. AMITABHA MUKHERJEE and Dr. IGOR V. LADNIK for their expert guidance and wise counsel without which this work couldn't have been possible. They patiently sat through the lengthy discussions which no doubt were stimulating and helped me very much in completing this work. I shall have fond memories of the time I spent with them.

Special thanks are also due to Prof. A. K. MALLIK, Prof. B. N. BANERJEE and Dr. PARTHA CHAKRABORTHY for their expert advice and timely help.

I am very grateful to my family members for giving me constant encouragement and motivating me to pursue graduate studies. Without their encouragement, I would not have reached this hallowed institution, leave alone completing my graduate studies.

I would be failing in my duty if I don't put on record my heart felt gratitude to my friends C. Ramesh (Trans.), Vidya Sagar, P.V.Ramakrishna, V.Durga Prasad, S. P. Chandrasekhar, N. Srinivas, U. V. Sarma, I. Sridhar and Boddapati, who gave me their love, shared my agonies and boosted my morale in times of hardship. I also enjoyed the company of Karanam Sekhar, Malladi Ravishankar, T. Suryaprakash, Mahesh (H-5), B. Venkateswara Rao (H-5) V. Srikanth,Phanikanth and Subrahmanyam.

Last but not the least I would like to express my gratitude to this venerable institution which gave me exposure to exciting problems in Mechanical Engineering. It also enabled me to hone up my skills to face the outside world with much better confidence. I thank Prof. S.G. Dhande and CAD-P for allowing me to take thesis print out.

M.V.R.

CONTENTS

LIST OF FIGURES

CHAPTER I

INTRODUCTION

Road humps are often used for controlling the speed of vehicles at sensible spots such as school zones, turning curves, residential areas etc. In order to keep vehicle speeds below the limiting speed, humps should be designed efficiently. Not much work has been carried out in this area to specify guidelines to the road designer for designing humps to control traffic. A good hump design should have minimal negative effect on the system at lower speeds and significant effect at higher speeds. How well can humps meet this goal?

Given a vehicle type, a desired speed limit, and a certain discomfort profile, what type of hump should a road designer use? This is the question we set out to answer. In order to model humps efficiently, one must know the class of vehicles for which the speed limits are to be enforced, the level of discomfort that can be withstood etc. Typical hump parameters include maximum height, maximum span, hump profile and the peak curvature rate. As it is not possible to construct and test all types of humps, simulation is done to identify the dynamic behavior of the system for travel across different types of humps.

This work has been divided into four chapters. In Chapter 1 various hump parameters that are to be considered are discussed. In Chapter 2, we discuss the different vehicle models. Our model which allows more degrees-of-freedom (8-DOF including driver) than the previous works [6] is also discussed. The solution methodology is also presented with 1-DOF model as an example. These measures are some what subjective e.g. [3, 7 and 14] have different views on these. Comfort charts have been derived for sustained vibrations; but the non-harmonic shock input of a hump does not fit this paradigm. On the other hand, breaking contact occurs quite frequently at microscopic scales and thresholds for sensible loss of contact are difficult to determine. The criteria for evaluating vehicle performance and passenger comfort and simulation results for various hump cases are dealt in Chapter 3. Concluding remarks along with scope for future work are embodied in Chapter 4. In Appendix A the elements of the model equation matrices are given. Two sample vehicle parameters representing a light vehicle like a passenger car (Make-1) and another medium size vehicle like a van (Make-2),are listed in Appendix B.

1.1 HUMP PARAMETERS

Dimensions and configurations of hump have a major influence on vehicle and driver. Generally a hump is specified by the following parameters.

1.1.1 HUMP PROFILE

The hump profile refers to the geometry of the hump. Such a profile can be circular (i.e., a segment of a circle), parabolic, cycloid, harmonic or connected segments of straight lines. Ideally a hump profile should at least have smooth entry and exit (characterized by zero end conditions i.e., zero height at ends and zero slopes at both ends and at mid point), and must be symmetric about the center line of its cross-section in order to produce the same effects while crossing it from either of its directions. For a given profile, the hump parameters are maximum height and span.

1.1.2 OTHER PROFILES

The following fourth order equation represents half of the hump section. It can be adapted according to the requirements of zero end conditions and to obtain desirable curvature.The main advantage of such a profile is that within the chosen length and height, a large variety of shapes can be generated by changing the curvature at the ends. The equation of a fourth order spline can be expressed as

$$Y_1(X) = a.X^4 + b.X^3 + c.X^2 + d.X + e \qquad \ldots\ldots (1)$$

with zero-end conditions i.e., $Y_1(0) = Y_1'(0) = Y_1'(L) = 0$, and with $Y_1(L) = H$, $Y_1''(0) = \varkappa$, we can relate the coefficients a, b, c, d and e of the above equation with hump parameters as,

$$a=(\varkappa L^2-6H)/2L^4, b=(4H-\varkappa)/L^3, c=\varkappa/2,$$
$$d = e = 0 \qquad \ldots\ldots (2)$$

where,

$\varkappa$ is the second derivative value at the end,

H is the maximum height of the hump,

L is half the maximum length of the hump,

$2L$ is the full span of the hump.

The equation of the other half of the hump can be derived on the similar lines and is found to be,

$$Y_2(x) = Y_1(2L - x) \qquad \ldots\ldots (3)$$

It must be noted that the value of $\varkappa$ be chosen such that the equation should not show peak heights larger than the maximum height of the hump chosen. The final shape of the hump can be expressed as follows;

$$Y(X) = \begin{cases} Y_1(X) & 0 \le X \le L \\ Y_1(2L - X) & L \le X \le 2L \\ 0 & \text{Otherwise} \end{cases} \qquad \ldots\ldots (4)$$

From the above equation it is to be understood that we are forcing the function to be zero outside the region [0, 2L]. Few shapes for various $\varkappa$ value, L and H are shown in Fig (1).

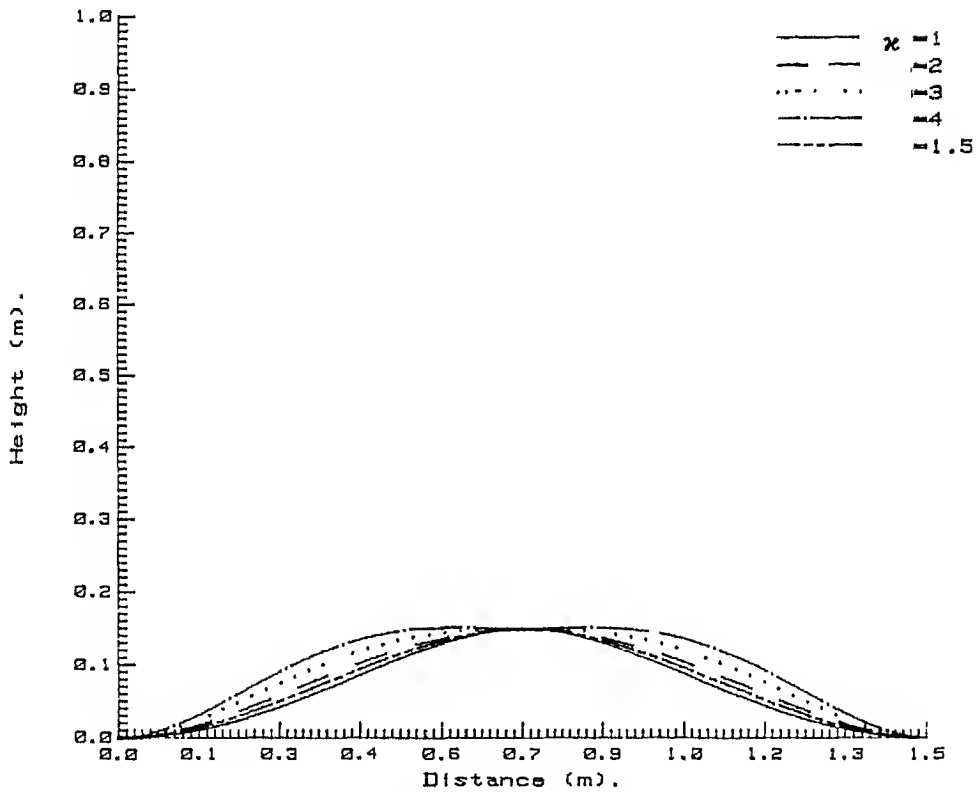

Fig. 1 Various hump sample profiles. Hump parameters are maximum span, maximum height, curvature at peak, smoothness at base, etc.

CHAPTER 2

MODEL DESCRIPTION

Next comes the question of choosing the valid vehicle model for simulating the results. In this chapter the various vehicle models along with present model, the input to the system, the solution methodology are discussed at length. The procedure is outlined for the simplest case of 1-DOF system.

2.1 VEHICLE MODELS

The simplest are quarter-car models which allow for only one dimensional, vertical (heave) motion, consisting of just the vehicle or sprung mass, is shown in Fig. 2. It is, moreover, a common practice to assume that the vehicle is moving with constant velocity V.

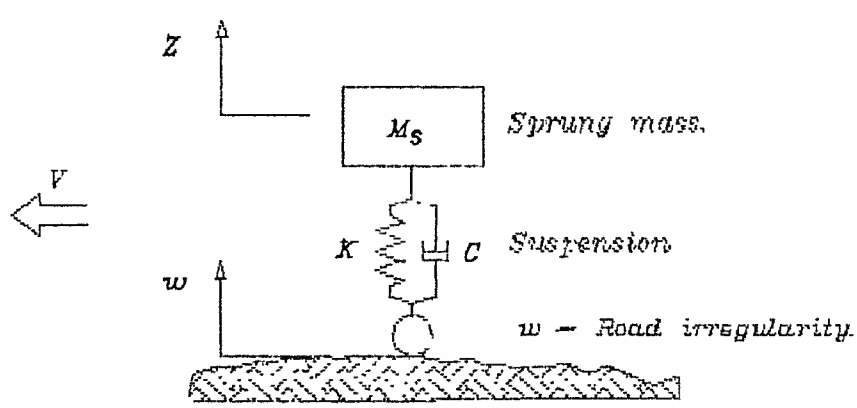

Fig. 2 One-degree-of-freedom vehicle model. This model can b analyzed theoretically and was used to validate our numerical model.

Adding a wheel/tire sub assembly (unsprung mass) to the above 1-DOF structure, leads to 2-DOF. quarter-car model (Fig. 3). The unsprung mass mode is often referred to as "wheel-hop," and is characterized by relatively light dampening and natural frequency between 8 and 12 Hz. The principal body mode, or sprung mass mode, is typically around 1 Hz.

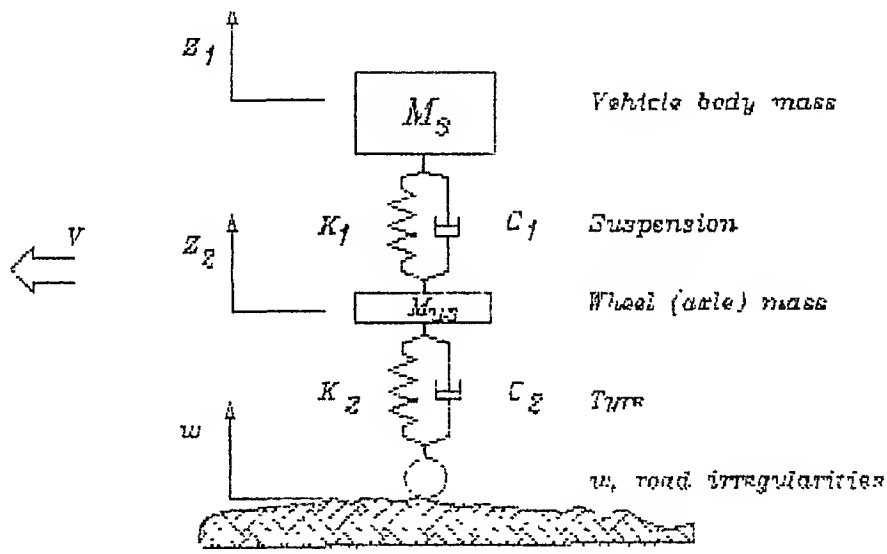

Fig. 3 Two-degree-of-freedom vehicle model.

Typical half car, 2-DOF models including front and rear wheels, model the pitch and heave of vertical modes (Fig. 4), often augmented by front and rear unsprung-mass vertical dynamics. Full

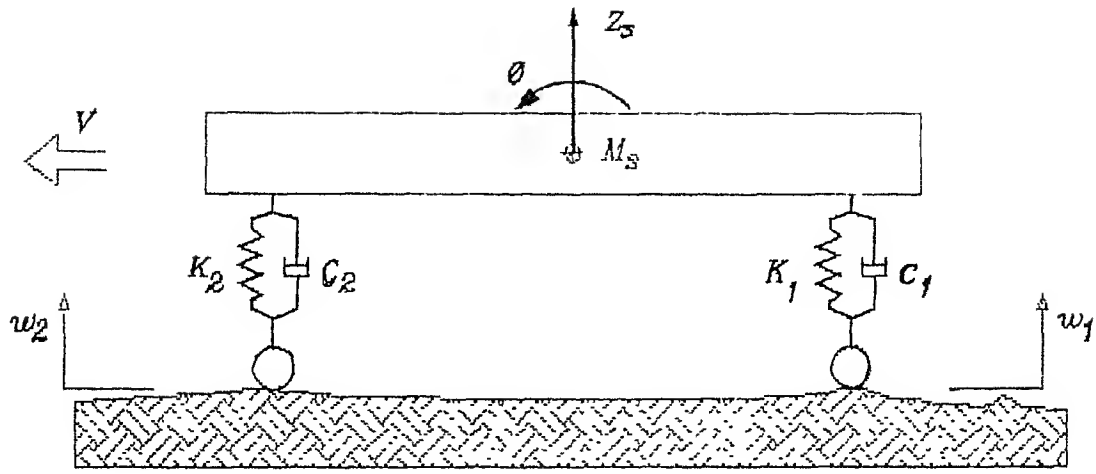

Fig. 4 Half-car 2-DOF model. This includes heave (Z-displacement of vehicle centre of mass) and pitch (longitudinal rotation of vehicle axis).

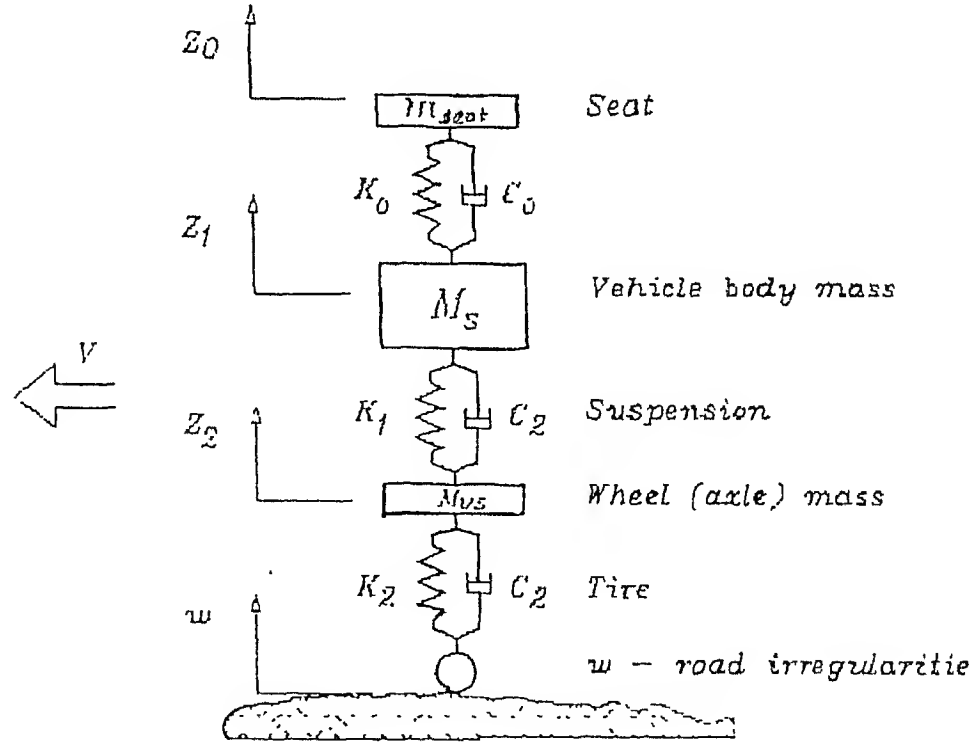

Fig. 5 Three-degree-of-freedom vehicle model (including seat). Passenger is assumed to be rigidly attached.

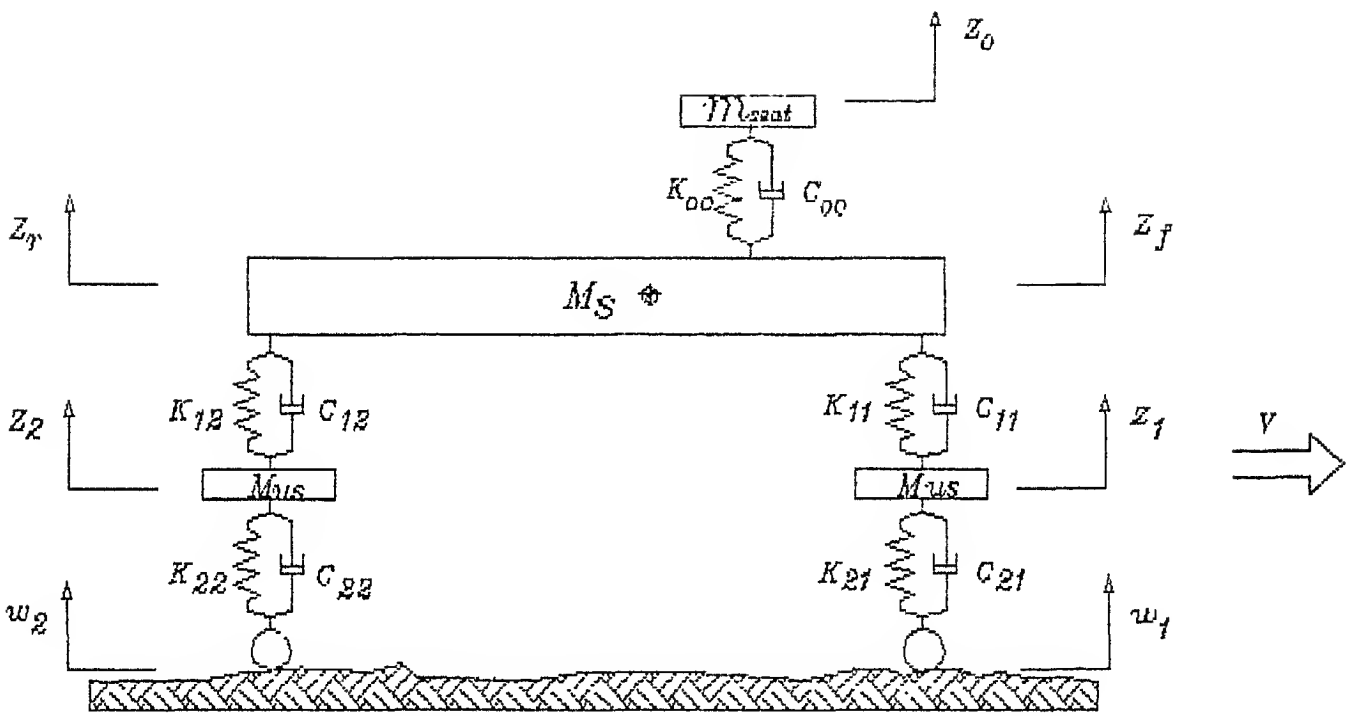

Fig. 6 Half-car-model including seat (5-DOF).

car, 3D models, on the other hand, include vehicle roll, as well as the pitch and heave modes (Fig. 7(a)). These models consider only rigid body motions, and are based on lumped-parameters, linearized dynamics. The suspension of a 2-DOF vehicle travelling on a randomly corrugated road was optimized with respect to both road holding and ride comfort by Dahlberg [3]. In this model the vehicle is subjected to stationary zero mean Gaussian random excitation. In the process of optimizing the elasto-damping elements of passenger car, Demic [5] adapted a 7-DOF vehicle model and reported a good match with the theoretical and experimental results. A 8-DOF model representing driver's seat also was studied by Pintado [4, 13] in both frequency and time domains for optimizing the suspension parameters. A 2-DOF vehicle model with active suspension system has been used for optimizing suspension parameters under different conditions [4, 9, 10, 11 and 16].

Several types of suspensions are used in the analysis and in the present work the passive suspensions is assumed. Suspension optimizing models are mostly linear with relatively small sprung mass velocities and displacement angles.

2.2 PRESENT MODEL

The present model assumes the following: The automobile model consists of a sprung mass, two independent front suspensions

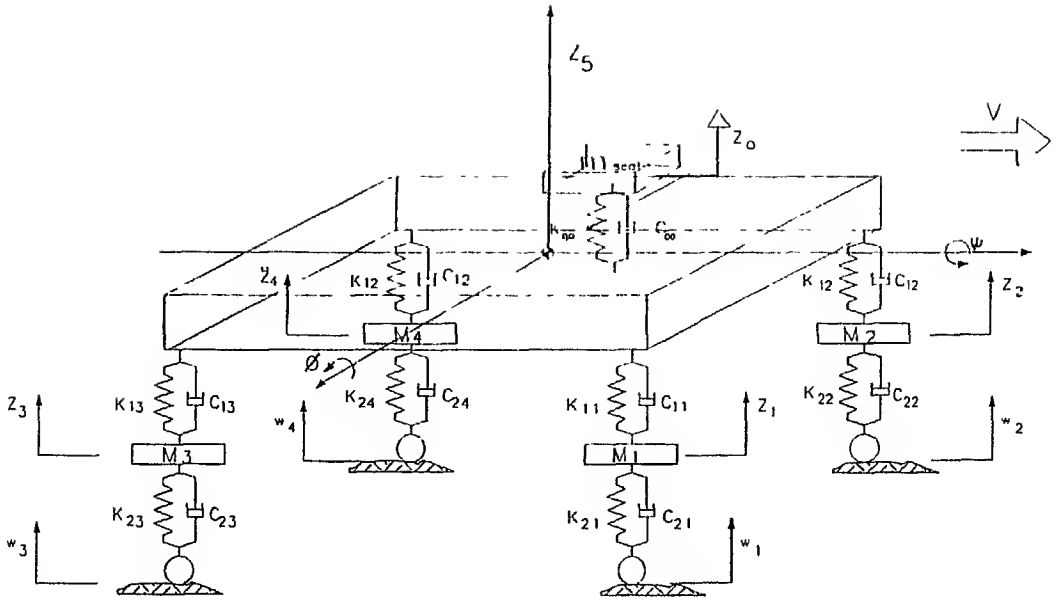

7(a)

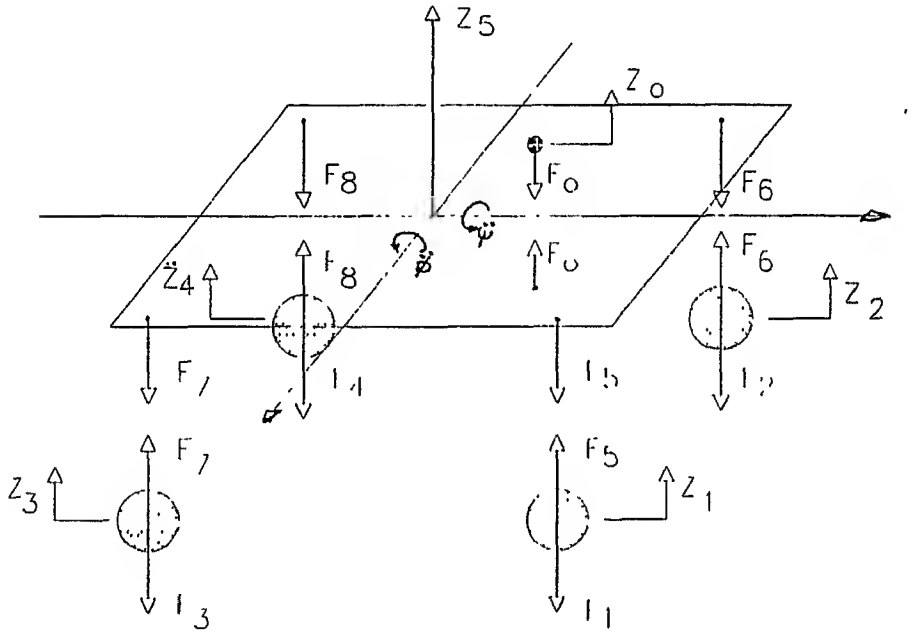

7(b)

Fig. 7(a) 8-DOF vehicle model.

7(b) Free-body-diagram of 8-DOF system.

between sprung and unsprung masses is assumed to consist of parallel combinations of springs and dampers. In addition, all mass assemblies are considered to be rigid bodies. The centers of mass of wheel suspension assembly is assumed at the wheel centers. In this model three degrees of freedom are associated with the sprung mass; bounce, roll and pitch. The bounce motion of all wheels relative to the sprung mass constitute four additional degrees of freedom. The vertical motion of driver's seat relative to the sprung mass constitute the last and the eighth degree of freedom of the vehicle. Aerodynamic forces acting on the vehicle are neglected.

The complexity of the 8-DOF model can be reduced to 5-DOF and 3-DOF models, for testing and validation, by shrinking the original 8-DOF model. For example, if we reduce the width of the 8-DOF model to zero then it represents 5-DOF model and if length is also made zero, it represents a 3-DOF model. This reduction to 3-DOF model and 5-DOF model was shown in Fig. 5 and Fig. 6 respectively. The 5-DOF model is the one adapted by Essam Kassem [6] for evaluating dynamic effect of speed control humps.

2.3 MATHEMATICAL FORMULATION OF 8-DOF VEHICLE MODEL

The mathematical formulation for 3D vehicle oscillations model presented below (Fig. 7(a)) makes it possible to analyze the

following:

a) Sprung mass vertical oscillations x5, roll ψ, and pitch ϕ

b) Wheel vertical oscillations x1, x2, x3 and x4

c) seat vertical oscillations x8

The oscillatory movements of the vehicle are caused by the excitation generated by the irregularities of the road which the tire fells at the road-tire contact point denoted by w1, w2, w3 and w4.

Characteristics of elasto-damping elements of the vehicle are described by means of the parameters $k(i,j)$, $c(i,j)$, $i = 1..4$, $j = 1..4$. Referring to Fig. 7(a), the following designations apply:

m1, m2 -unsprung masses of the front wheel,

m3, m4 -unsprung masses of the rear wheel,

m5 -sprung mass,

mo -mass of driver's seat including driver,

Ir, Ip -mass moment of inertias of the sprung mass about roll and pitch axes,

l_1, l_2, S -coordinates of the center of mass of the seat with reference to sprung mass center.

Taking into account possible degrees of freedom in the vehicle

model adapted, the following relations are developed to define deformations of the elastic elements:

$$
\begin{aligned}
D_0 &= x_5 - l_y.\phi + l_x.\psi \\
D_1 &= x_5 + l_1.\phi - S.\psi - x_1 \\
D_2 &= x_5 + l_1.\phi + S.\psi - x_2 \\
D_3 &= x_5 - l_2.\phi - S.\psi - x_3 \\
D_4 &= x_5 - l_2.\phi + S.\psi - x_4 \qquad \ldots\ldots (5) \\
D_5 &= x_1 - w_1 \\
D_6 &= x_2 - w_2 \\
D_7 &= x_3 - w_3 \\
D_8 &= x_4 - w_4
\end{aligned}
$$

Relative velocity of the shock absorber is defined by means of the following expressions:

$$
\begin{aligned}
D_{00} &= \dot{x}_5 - l_y.\dot{\phi} + l_x.\dot{\psi} \\
D_9 &= \dot{x}_5 + l_1.\dot{\phi} - S.\dot{\psi} - \dot{x}_1 \\
D_{10} &= \dot{x}_5 + l_1.\dot{\phi} + S.\dot{\psi} - \dot{x}_2 \\
D_{11} &= \dot{x}_5 - l_2.\dot{\phi} - S.\dot{\psi} - \dot{x}_3 \\
D_{12} &= \dot{x}_5 - l_2.\dot{\phi} + S.\dot{\psi} - \dot{x}_4 \qquad \ldots\ldots (6) \\
D_{13} &= \dot{x}_1 - \dot{w}_1 \\
D_{14} &= \dot{x}_2 - \dot{w}_2 \\
D_{15} &= \dot{x}_3 - \dot{w}_3 \\
D_{16} &= \dot{x}_4 - \dot{w}_4
\end{aligned}
$$

The following relations are developed to obtain the the forces in the linear elasto-damping elements:

a) Tires:

$$F_1 = k_{21}.D_5 + c_{21}.D_{13}$$

$$F_2 = k_{22}.D_6 + c_{22}.D_{14}$$

$$F_3 = k_{23}.D_7 + c_{23}.D_{15} \qquad \text{..... (7)}$$

$$F_4 = k_{24}.D_8 + c_{24}.D_{16}$$

b) Suspension springs and shock absorbers:

$$F_5 = k_{11}.D_1 + c_{11}.D_9$$

$$F_6 = k_{12}.D_2 + c_{12}.D_{10}$$

$$F_7 = k_{13}.D_3 + c_{13}.D_{11} \qquad \text{..... (8)}$$

$$F_8 = k_{14}.D_4 + c_{14}.D_{12}$$

c) Driver seat's elastic elements:

$$F_o = k_{oo}.D_o + c_{oo}.D_{oo} \qquad \text{..... (9)}$$

On the basis of the force scheme depicted in Fig. 7(b), and invoking Newton's laws, one can write the following differential equations describing small oscillatory motions of the vehicle model around the equilibrium position:

$$\ddot{x}_0 = (F_0)/m_0$$

$$\ddot{x}_1 = (F_5 - F_1)/m_1$$

$$\ddot{x}_2 = (F_6 - F_2)/m_1$$

$$\ddot{x}_3 = (F_7 - F_3)/m_2 \qquad \text{..... (10)}$$

$$\ddot{x}_4 = (F_8 - F_4)/m_2$$

$$\ddot{x}_5 = -(F_5 + F_6 + F_7 + F_8 - F_0)/m_5$$

$$\ddot{x}_6 = (F_5 + F_7 - F_6 - F_8 - F_0 . l_x)\ S/I_r$$

$$\ddot{x}_7 = ((F_7 + F_8) . l_2 - (F_5 + F_6) . l_1 + F_0 . l_y)/I_p$$

F_1 through F_4 are the contact forces. When these go to zero, the car loses contact, where these equations are no longer valid. However numerically, such loss of contact is difficult to determine exactly. These equilibrium equations can be put in the most general form of the second order linear differential equations as [8, 12 and 13],

$$[M]\{\ddot{X}(t)\} + [C]\{\dot{X}(t)\} + [K]\{X(t)\} = \{F(t)\} \qquad \text{..... (11)}$$

Where [M], [C] and [K] are the inertia, damping and stiffness matrices respectively; matrices [C] and [K] might show non-linear character of the dampers and springs; $\{X\}$, $\{\dot{X}\}$ and $\{\ddot{X}\}$ are the displacement, velocity and acceleration vectors in generalized coordinates of the multi body assemblage and the load vector $\{F(t)\}$ is due to road irregularities, to braking forces and to centrifugal forces generated when the vehicle runs on a curved track.

The detailed description of these equations, elements of matrices and force vector for the case of the present vehicle model are presented in Appendix A. The model parameters are presented in Appendix B, for two vehicle types.

2.5 SOLUTION METHODOLOGY

2.5.1 TIME DOMAIN SOLUTION

The above equations can be solved in both time and frequency domains using numerical methods. For getting time-domain solution Runge-Kutta method is used. For frequency domain solution Transfer Function approach is adapted. The state space representation of above equations yields,

$$\begin{Bmatrix} \{\dot{X}_1\} \\ \{\dot{X}_2\} \end{Bmatrix} = \begin{bmatrix} [O] & [I] \\ -[M]^{-1}[K] & -[M]^{-1}[C] \end{bmatrix} \begin{Bmatrix} \{X_1\} \\ \{X_2\} \end{Bmatrix} + \begin{Bmatrix} \{0\} \\ -[M]^{-1}\{F(t)\} \end{Bmatrix} \quad \ldots \quad (12)$$

or in the most general form,

$$\{\dot{X}(t)\} = [A]\{X(t)\} + [B]\{U(t)\} \quad \ldots\ldots \quad (13)$$

Where,

$\{X\}$ is the vector of state variables,

$\{X_1\}$ contains the generalized coordinates, both rotational and translational,

$\{X_2\}$ is the first time derivative of vector $\{X_1\}$,

$\{\dot{X}_1\}$ is the first time derivative of vector $\{X_1\}$,

$\{\dot{X}_2\}$ is the second time derivative of vector $\{X_1\}$,

$\{U(t)\}$ is the input vector.

2.5.2 FREQUENCY DOMAIN SOLUTION

The frequency domain solution can be obtained by following state space approach as follows. The solution to (13) can be assumed as

$$\{Y(t)\} = [A]\{X(t)\} + [D]\{U(t)\} \qquad \text{..... (14)}$$

Taking Laplace Transforms of both equations (13, 14) we get,

$$s\{X(s)\} - \{X(0)\} = [A]\{X(s)\} + [B]\{U(s)\}$$

$$\{Y(s)\} = [C]\{X(s)\}$$

with zero initial conditions i.e., $\{X(0)\} = \{0\}$, we get

$$s\{X(s)\} = [A]\{X(s)\} + [B]\{U(s)\}$$

$$\{Y(s)\} = [C]\{X(s)\}$$

solving for $\{X(s)\}$, the above equation give

$$\{X(s)\} = (s[I] - [A])^{-1}[B]\{U(s)\}$$

and

$$\{Y(s)\} = [C](s[I] - [A])^{-1}[B]\{U(s)\}$$

or,

$$\{Y(s)\} = [[G(s)]\{U(s)\}] \quad \ldots\ldots (15)$$

where,

$$[G(s)] = [[C](s[I] - [A])^{-1}[B]] \quad \ldots\ldots (16)$$

is the Transfer Function matrix defined as the ratio of Laplace Transform of output to that of input. And,

s is a complex quntity and is equal to $j\omega$ where $j = \sqrt{-1}$, and ω is the angular frequency expressed in rad/sec, $\omega = 2\pi f$, f is the frequency in Hz,

$[I]$ is the unit matrix,

$[0]$ is the zero matrix,

$\{U(s)\}$ is the Laplace Transform of input i.e., $\mathfrak{L}(U(t))$

$\{Y(s)\}$ is the Laplace Transform of output i.e., $\mathfrak{L}(Y(t))$

$\{X(s)\}$ is the Laplace Transform of $X(t)$

$[C]$ is a matrix, in the present case it is unity.

Because [C] is unity, $\{X(s)\} = \{Y(s)\}$.

This transfer function, as seen, is a constant function of s for the given system and therefore it is a constant function of s as long as the system is time invariant i.e., the system parameters does not change with time. It is independent of input to the system. The output of the system coordinates in frequency domain can be obtained from (15).

2.5.3 TIME DOMAIN INPUT

Assuming the vehicle velocity is not affected by the road geometry, front and rear tire inputs ((w_1, w_2) and (w_3, w_4)) are related by the following expressions:

$$w_1, w_2 = Y_1(t) \qquad \ldots\ldots (17)$$

and,

$$w_3, w_4 = Y_2(t-\tau) \qquad \ldots\ldots (18)$$

Where the time delay τ depends on the the wheel base and vehicle running velocity (V).

$$\tau = \frac{\text{Wheel-base}}{V} = \frac{W}{V} \qquad \ldots\ldots (19)$$

Therefore the input to the front and rear tires in time domain can be expressed as,

$$w_1 = Y(t) = \begin{cases} Y_{11} = A(t-t_o)^4 + B(t-t_o)^3 + C(t-t_o)^2, & t_o \le t \le L/V + t_o \\ Y_{12} = A(t_1-t)^4 + B(t_1-t)^3 + C(t_1-t)^2, & L/V \le t \le 2L/V \\ Y_{13} = 0 & \text{Otherwise} \end{cases}$$

and $w_3 = Y(t - \tau)$

$$= \begin{cases} Y_{21} = A(t-t_2)^4 + B(t-t_2)^3 + C(t-t_2)^2, & W \le t \le (W+L)/V \\ Y_{22} = A(t_3-t)^4 + B(t_3-t)^3 + C(t_3-t)^2, & (W+L)/V \le t \le (W+2L)/V \\ Y_{23} = 0 & \text{Otherwise} \end{cases}$$

..... (20)

Where,.

$A = a V^4$, $B = b V^3$, $C = c V^2$. (a, b, c are defined in (2)),

$W = l_1 + l_2$ is the wheel-base of the vehicle,

$t_o \ge 0$, is the time taken by the car to reach the bump,

$t_1 = t_o + 2L/V$, $t_2 = t_o + W/V$, $t_3 = t_o + (W + 2L)/V$,

V is the forward velocity of the vehicle.

2.5.4 FREQUENCY DOMAIN INPUT

To calculate the input vector {U(t)} in frequency or s domain, we need to consider the Laplace transform of {U(t)} and here for the inputs w_1, w_2, w_3, w_4 the Laplace transforms are as follows:

$$W_1(S),\ W_2(S) = \mathcal{L}(Y(t)) = \int_0^{\infty} Y(t).e^{-St}dt$$

$$= \int_{to}^{(to+L/V)} Y_{11}(t).e^{-st}dt + \int_{L/V}^{(2L/V)} Y_{12}(t).e^{-St}dt \qquad \ldots\ldots (21)$$

and,

$$W_3(S),\ W_4(S) = \mathcal{L}(Y(t-\tau)) = \int_0^{\infty} Y(t-\tau).e^{-St}dt$$

$$= \int_{t2}^{(t2+L/V)} Y_{11}(t).e^{-st}dt + \int_{(t2+L/V)}^{(t2+2L/V)} Y_{12}(t).e^{-St}dt \qquad \ldots\ldots (22)$$

from first shifting property of Laplace transforms, W_3 can be expressed as,

$$W_3(S),\ W_4(S) = e^{-S\tau}.\mathcal{L}(Y(t)) = e^{-S\tau}.W_1(S) \qquad \ldots\ldots (23)$$

2.6 TRANSFER FUNCTION FOR 1-DOF VEHICLE MODEL CASE

The transfer function approach for obtaining frequency domain solution for the case of 1-DOF vehicle is explained below. The governing dynamic equilibrium equation for the vehicle model shown in Fig. 2 can be written as,

$$m\ddot{z} + c\dot{z} + kz = kw + c\dot{w} \qquad \ldots\ldots (24)$$

Where,

m = M_s is the sprung mass (Kg),

k = K_1 is the suspension spring constant (N/m),

c = C_1 is the suspension damping rate (N-sec /m),

z, $\dot{z}$, $\ddot{z}$ are displacement, velocity and acceleration of mass m,

($\cdot$ dot indicates derivative with respect to time),

w indicates the input excitation to the system (road irregularities).

Transforming this equation into state space representation, the matrices in (12) represents,

$$[A] = \begin{bmatrix} 0 & 1 \\ -k/m & -c/m \end{bmatrix}_{2x2} \quad [B] = \begin{bmatrix} 0 & 0 \\ k/m & c/m \end{bmatrix}_{2x2} \quad \text{and} \quad \{U(t)\} = \begin{Bmatrix} w \\ \dot{w} \end{Bmatrix}_{2x1}$$

and the state vector $\{X\}$ is $[\ \dot{z} \quad \ddot{z}\ ]^T_{2x1}$

$$\therefore T.F = [G] = [s.I - A]^{-1}[B]$$

$$= \begin{bmatrix} k/m & c/m \\ s.k/m & s.c/m \end{bmatrix} \frac{1}{\Delta} = \begin{bmatrix} G_{11} & G_{12} \\ G_{21} & G_{22} \end{bmatrix}$$

$$\{Y(s)\} = [G]\ \{U(s)\} = \begin{Bmatrix} k/m\ w(s) + c/m\ \dot{w}(s) \\ s(k/m\ w(s) + c/m\ \dot{w}(s)) \end{Bmatrix} \frac{1}{\Delta}$$

where Δ is the determinant of [G] and is equal to,

$$\Delta = s^2 + s.c/m + k/m$$

Displacement of mass m,

$$z(s) = Y_1(s) = (k/m.w(s) + c/m.\dot{w}(s)) / \Delta$$

If $w(t) = A_o \sin(\omega.t)$ then,

$$w(s) = \mathfrak{L}(w(t)) = \mathfrak{L}(\sin(\omega.t)) = \frac{A_o.\omega}{(\omega^2 + s^2)}$$

and

$$\dot{w}(s) = \mathfrak{L}(\dot{w}(t)) = \mathfrak{L}(\omega.\cos(\omega.t)) = \frac{A_o.\omega.s}{(\omega^2 + s^2)}$$

then $z(s)$ is given by,

$$z(s) = \frac{A_o/m\ (k + c.s)/(\omega^2 + s^2)}{\Delta}$$

The transfer functions G_{11}, G_{12} for this system case are shown in Fig. 8(a) and the corresponding input in s domain is shown in Fig. 8(b) and the resulting output in s domain is given in Fig. 8(c).

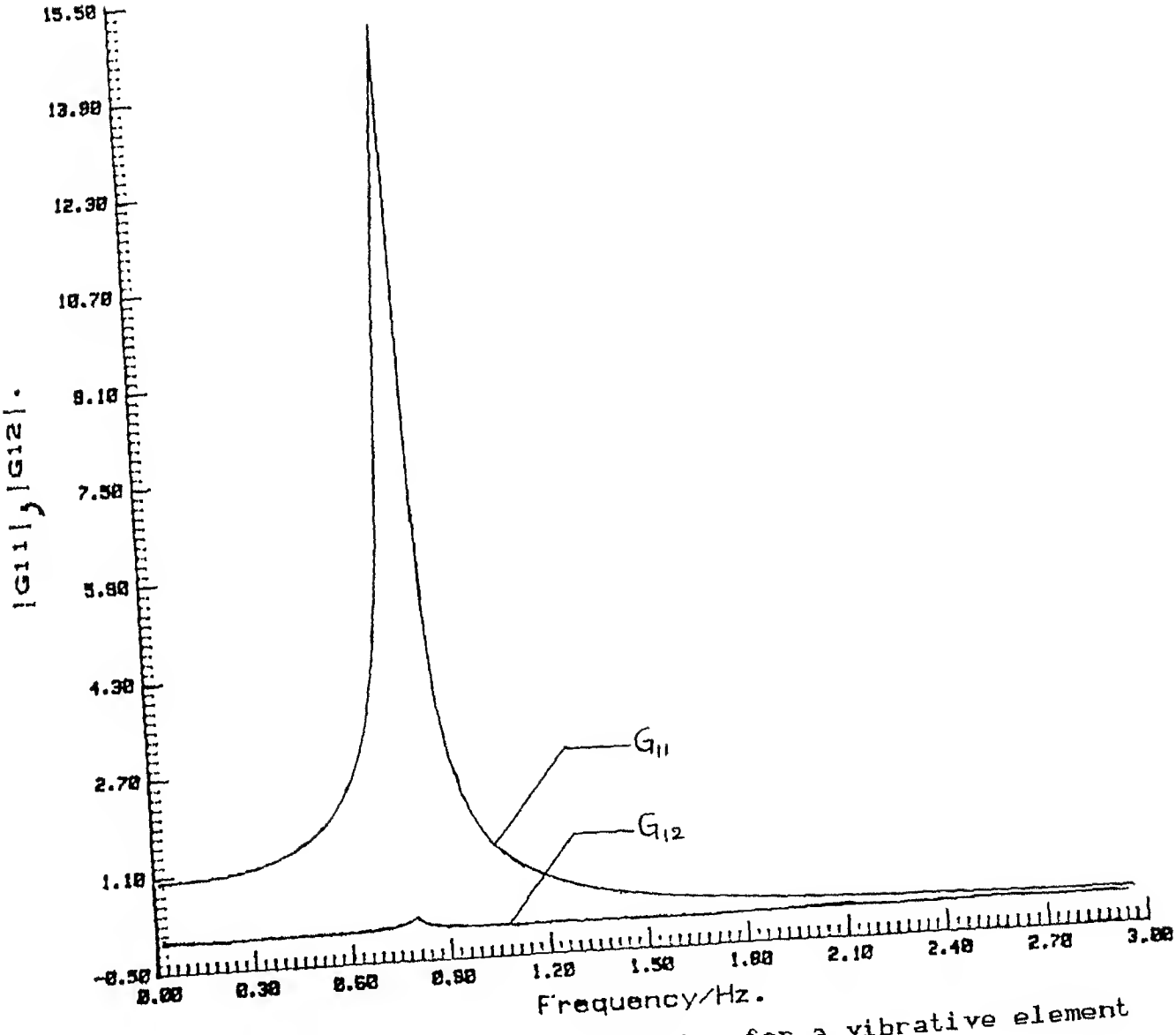

Fig. 8(a) Magnitude of transfer function for a vibrative element shown in Fig. 2.

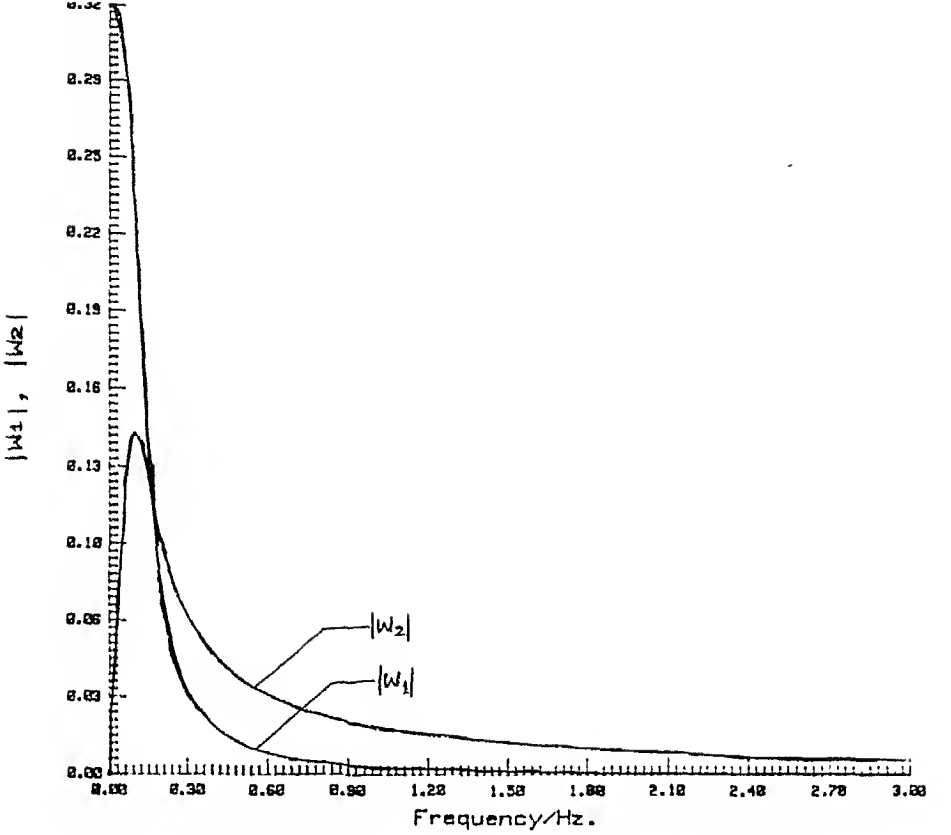

Fig. 8(b) Magnitude of input for the vibrative element shown in Fig. 2.

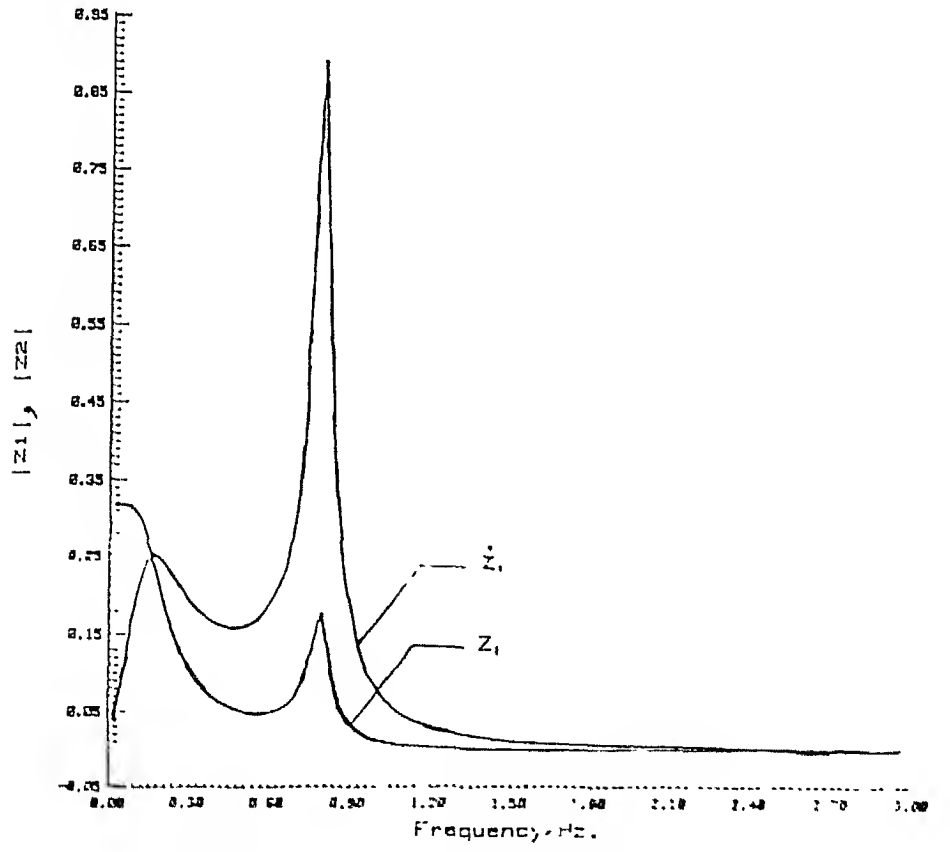

Fig. 8(c) Magnitude of output for the vibrative element shown in Fig. 2.

C H A P T E R III

HUMP SELECTION - A DISCUSSION

Now the question is "What are the suitable parameters of a hump that best meets the objectives, if the limiting speed and the vehicle type are specified?" Considering the conflicting factors viz. road-holding and ride comfort, as evaluated by conducting tests on level roads, it is not possible to directly use them for case of travel across a hump in evaluating the *acceptability* of the hump. As no test data is available regarding these factors, in this work, the dependency of the dynamic response of vehicle and driver on road sections with hump is presented.

In this chapter the general criteria for evaluating the performance of vehicle and driver are discussed. The criterions modeled in this thesis are described. Simulation results are presented in the form of graphs for various travel considerations of vehicle across different humps.

3.1 ROAD HOLDING PROPERTY

Optimal road holding can be seen as the minimal probability that the magnitude of road-wheel contact force will be larger than a given level. When a vehicle crosses a hump at a speed, for safety, the tire should not lose contact with the ground. This phenomena of

contact loosing can be quantified best with the road-wheel contact force (7). It can be seen that these forces (7) are proportional to the tire vertical displacement and velocity. Under severe cases, the wheels can be deflected by large amounts causing damage to suspension. The contact forces $F_i (i=1,4)$ in equation (7) are deviations from the nominal contact force due to the weight of the vehicle. Thus, even if F_i is negative, so long as $(F_i + P_i)$ is positive, contact is not lost. P_i is the total load share on any tire (For example in Fig. 19, assuming $P_i = W/4$ on each tire, the contact force is negative only marginally).

To select a hump from this criteria and result given in this work, one have to have a limiting load on the tire. If at all one wishes to select a hump from these results, he has to decide himself the allowable/acceptable limits of these factors. For example, if we limit ourself that the wheel-road contact force should not be more than 1.75 times that in static condition when the vehicle crosses the hump, for the vehicle Make-1 presented in Appendix B, then the assumed velocity at which contact is lost can be seen to be 6 m/sec (21.5-KM PH) (Figures 37 and 38).

3.2 HUMAN COMFORT

With human comfort point of view, an ideal hump should be such that at and below the limiting speeds ride is to be comfortable and vice-versa. There are many a different ways to quantify the *ride quality*. The simplest one is based on the calculation of the root-mean-square(rms) value of the vertical acceleration typically measured at the driver's or passenger's seat location. A useful early study in this regard was published in 1978 [14]. The authors draws conclusions based on field study, states that "the values of these magnitude weighted rms values will range roughly from 0 to 0.04g for smooth(interstate highway) rides, 0.04 to 0.06g for medium rides, and above 0.06g for rough rides."

The rms quantifiers do not reflect the frequency dependence of human sensitivity to vibrations. To account for this aspect of ride comfort, the International Standard Organization (ISO) has developed a standard , which considers the duration of human exposure to the vibrations (ISO 2631). According to the above standard, the region of greatest human sensitivity to vertical vibrations lies between 4 and 8 Hz, which roughly include various resonance frequencies of human internal organs. The above measures are primarily based on decoupling the degrees of freedom typically performed in only one direction at a time. It is not clear the sustained input models such as these would apply to non periodic and

shock loading conditions as in a road hump. To select a hump from this criteria and simulation results presented here, one have to have a limiting/tolerable acceleration limits which can be directly comparable. Here, frequency dependency of vertical acceleration and displacement at driver's seat location are also simulated because, if at all any text is going to be conducted for this case, it would be easy to measure and compare these quantities.

3.3 OTHER ASPECTS

One often introduces a constraint in the form of rms suspension stroke or so called *rattle space*. Rattle space is a term used to indicate the clearance allowed for the vertical movement of wheel. High rattle space indicates the possible touching of the axle with the chassis or the car body, causing possible damage. This aspect is important for case of travel across a hump because, there may be a possible large and sudden deflection of suspension which may damage vehicle itself. This aspect is very significant for designing suspension, here it is only considered to study the variation of the packaging constraints.

3.4 PRESENT MODEL ACCEPTANCE CRITERIA

In the present work the following performance criteria has been modeled which are being widely adopted for various purposes of

evaluating the vehicle performance [1, 2, 3, 4, 6, 9, 10, 11, 13, 14, 15 and 16]. In time domain,

a). Vertical acceleration at drivers's seat (related to ride comfort).

b). Suspension working stroke or rattle space (related to packaging constraints of the vehicle body).

c). Road-wheel contact force variation (related to road holding property).

and in frequency domain,

d). Vertical acceleration of the driver.

e). Vertical displacement of the driver.

From Fig. 9, it is clear that as vehicle velocity is exceeding certain value, the rms vertical acceleration of driver is decreasing indicating a good drive comfort. This encourages the motorists to travel at much higher speeds and the hump in question is becoming a overhead. This figure also compares two types of vehicles, one with larger mass (Make-2) and the other with lesser mass (Make-1). It is clear that the vehicle with larger mass is having much higher dynamic effects at a given speed compared to the lesser weight one.

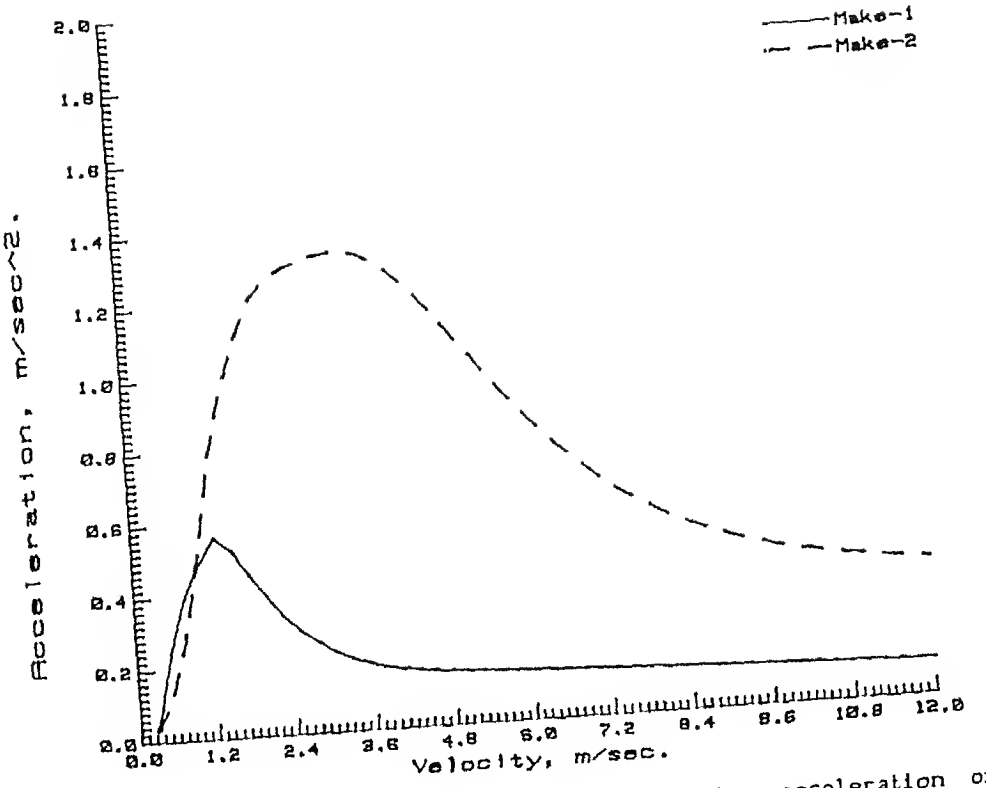

Fig. 9 Effect of crossing speed on the rms vertica acceleration of driver. (Make-1 and Make-2 refer to vehicle data). This result indicates that the vehicles with larger mass undergo comparitively greater dynamic effects

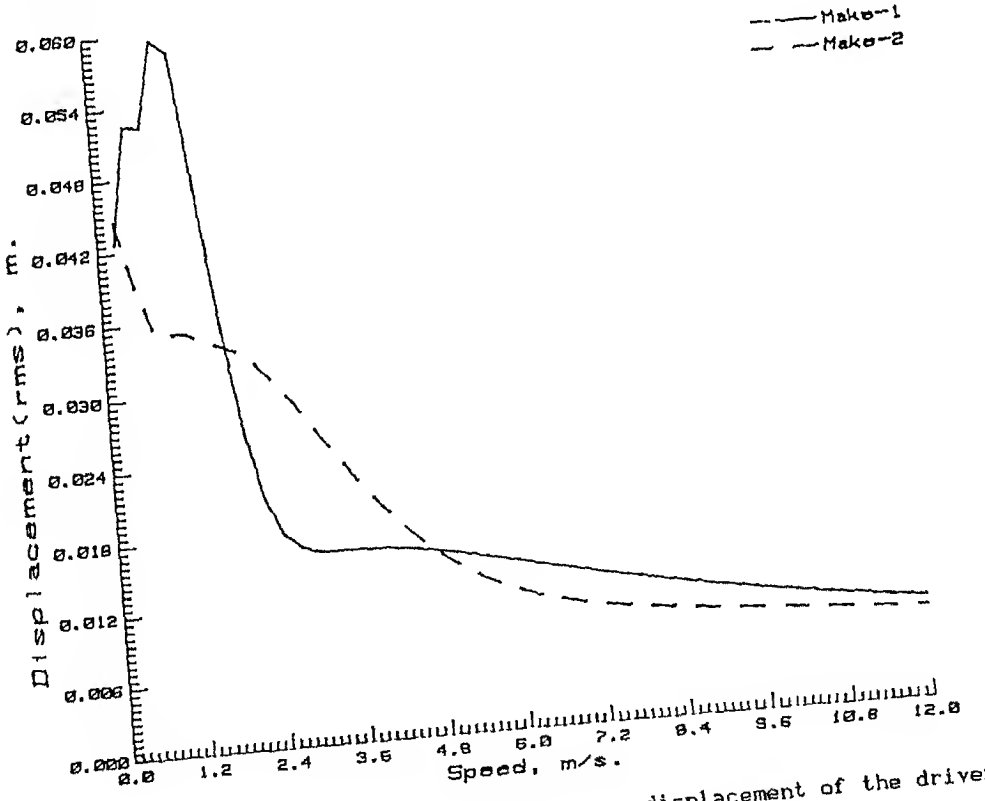

Fig. 10 Effect of crossing speed on the rms displacement of the driver (Make-1 and Make-2 refer to vehicle data).

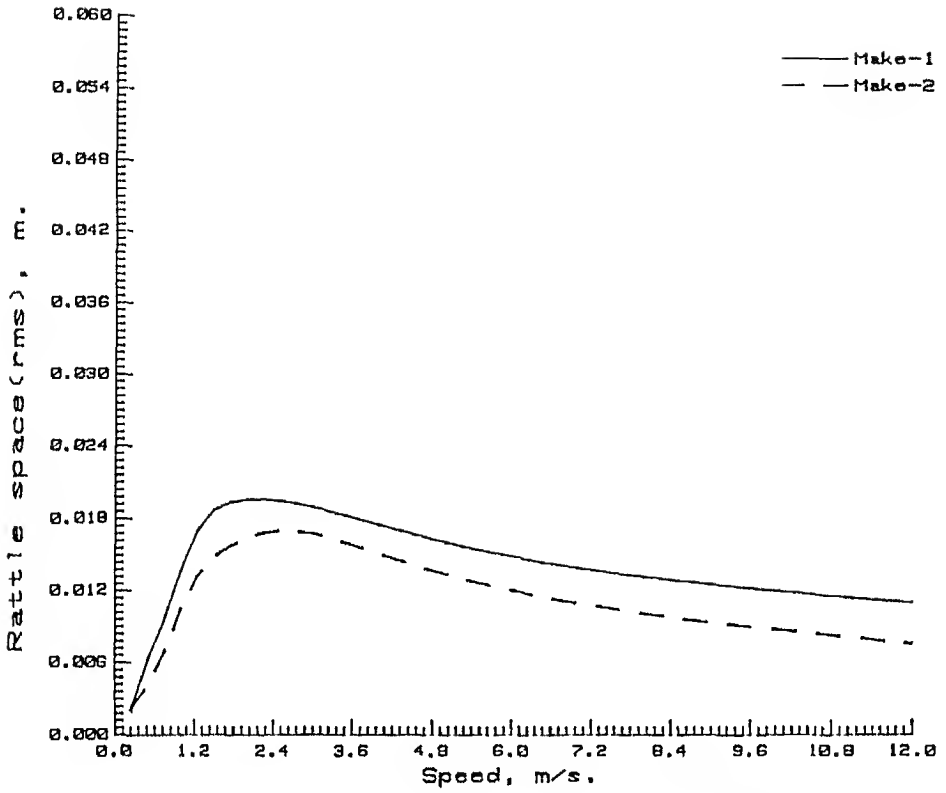

Fig. 11 Effect of crossing speed on the rms rattle at front end.

(Make-1 and Make-2 refer to vehicle data).

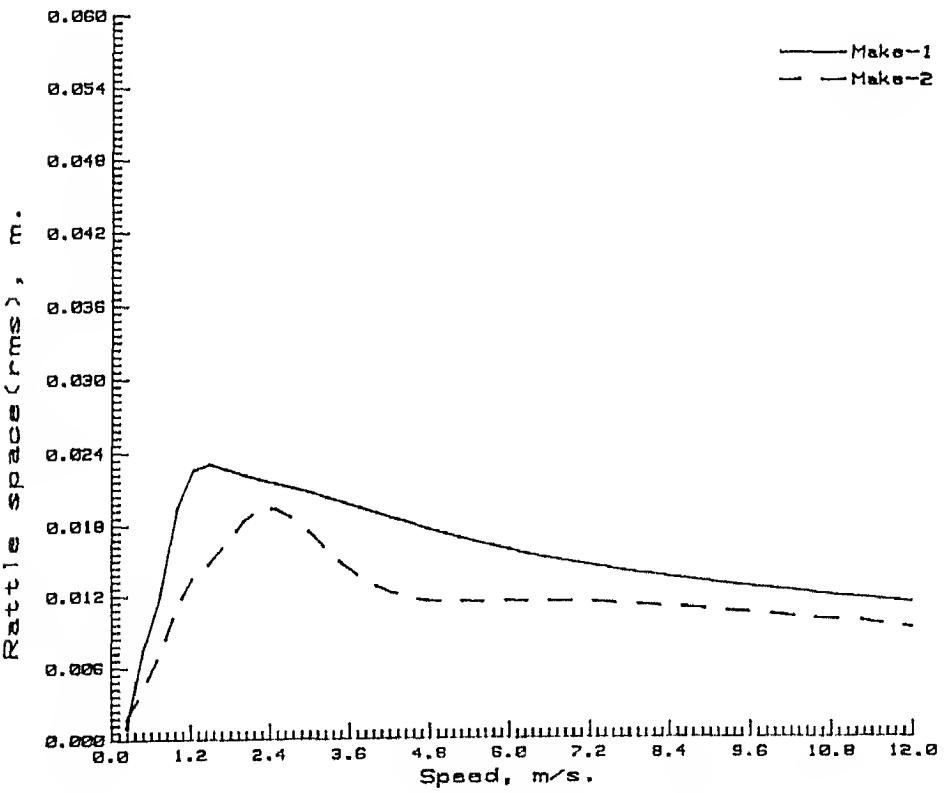

Fig. 12 Effect of crossing speed on the rms rattle at rear end.

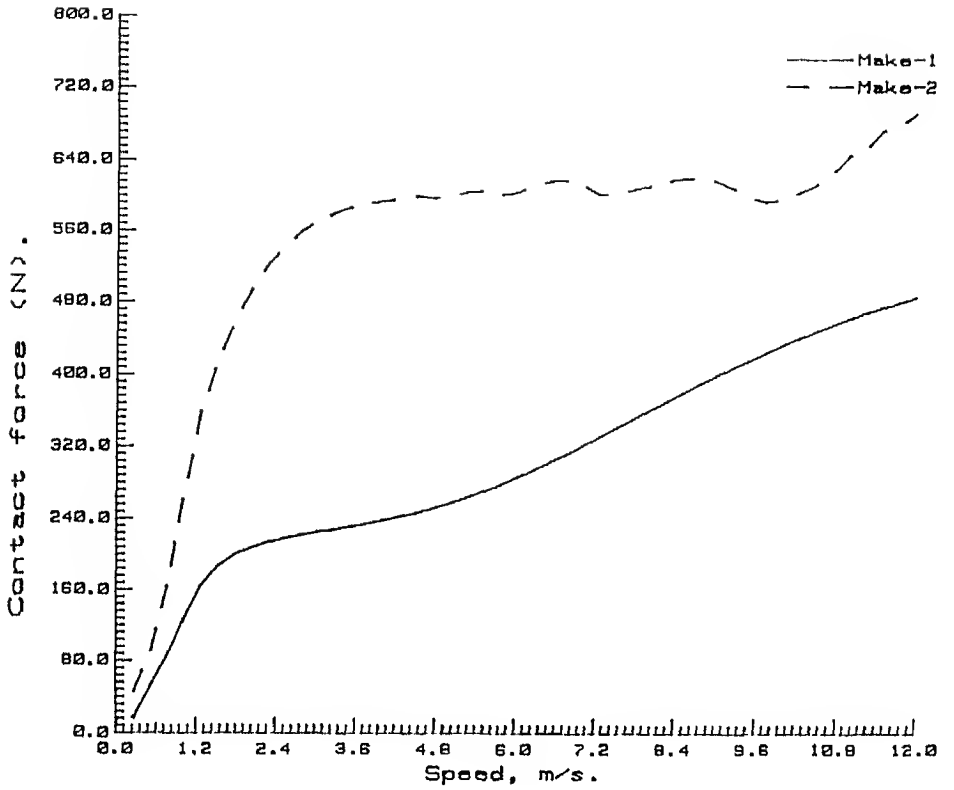

Fig. 13 Effect of crossing speed on the rms road wheel contact force at front end. (Make-1 and Make-2 refer to vehicle data). This result indicates that road holding force is higer for vehicles with larger mass. These are deaviations from nominal values due to the vehicle weight.

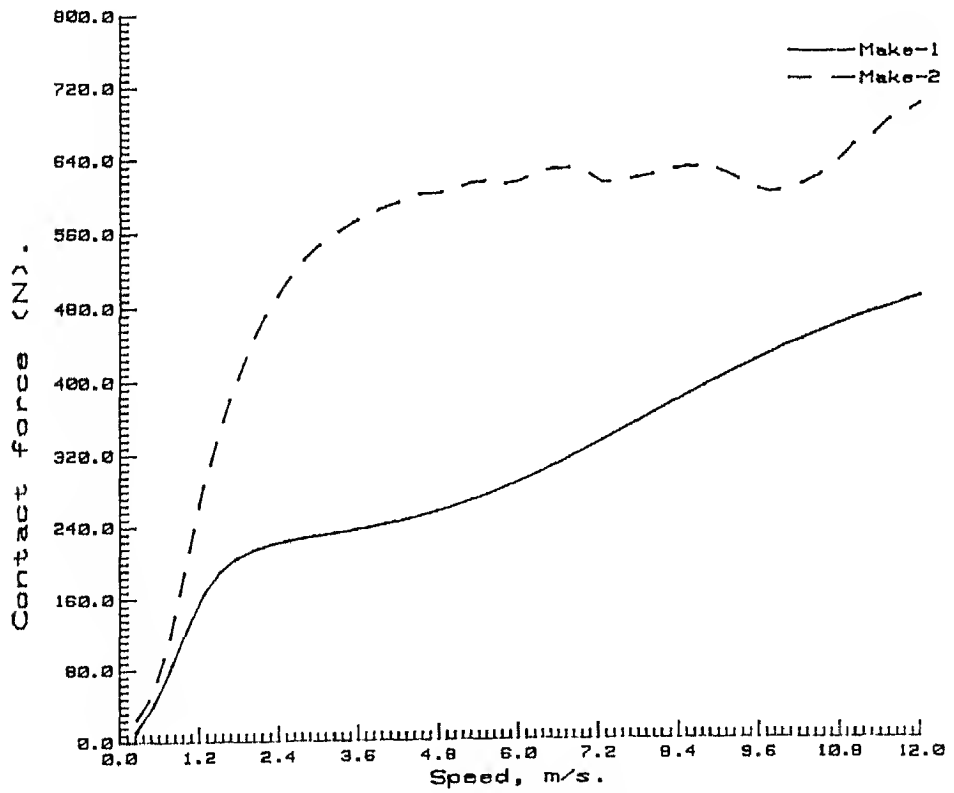

Fig. 14 Effect of crossing speed on the rms road wheel contact force at rear end. (Make-1 and Make-2 refer to vehicle data).

Fig. 10 displays rms vertical displacement of the driver. This displacement is also decreasing beyond certain velocity level. Figures 11 and 12 show that the rms *rattle space* is also decreasing with increasing speed, and this magnitude is higher for lesser mass car than the other. On the other hand, the rms wheel-road contact forces show an increasing effect with velocity. That means this contact force may cross the permissible limit and thus may not satisfy road-holding criterion. Often it may be possible from these plots to draw the fly-off velocity assuming assuming the limit value of the contact force. Moreover, large mass vehicles experience relatively large contact forces and is very likely to loose contact at lower velocities compared to lesser mass vehicles.

3.5 EFFECT OF VARYING THE WIDTH OF THE HUMP

Five different hump widths are examined. These are: 1.0, 1.25, 1.5, 1.75 and 2.0 m. Here hump height(0.15 m) and crossing velocity(5.0 m/s) are kept constant. Figures 15-20 show the effect of varying the width of the hump on the various aspects discussed in the previous section. A general conclusion can be drawn upon examining the response figures which say that the wider the hump the more is the dynamic effect on driver and the rattle space. Where a tensile part of the road holding force is decreasing making the drive safe.

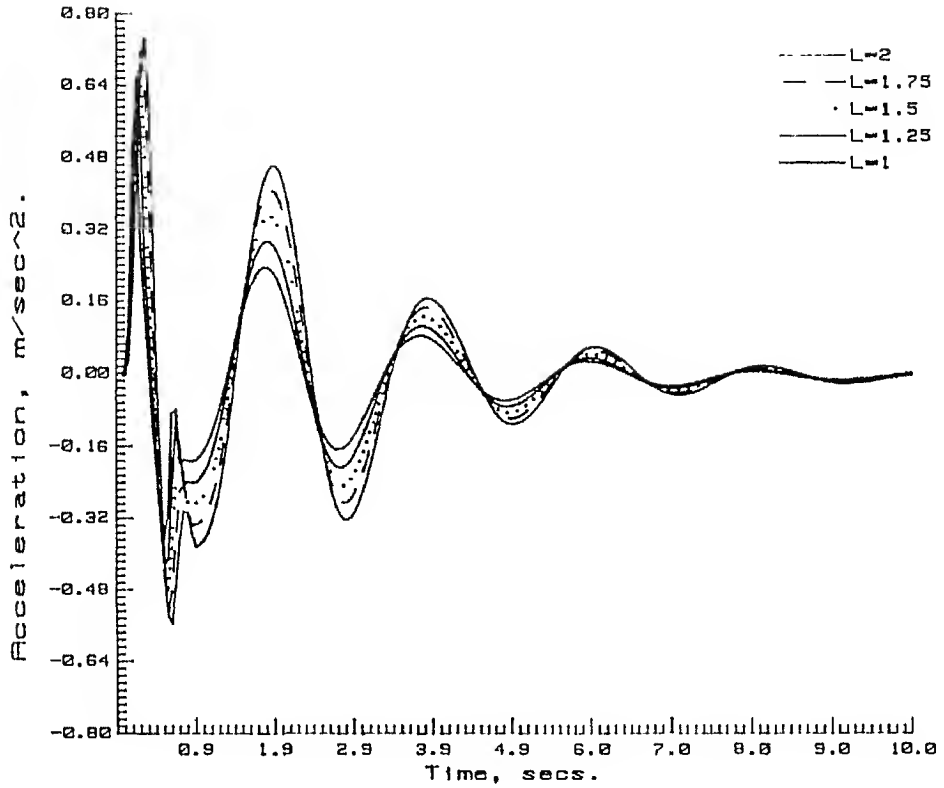

Fig. 15 Effect of varying the width of the hump on the acceleration of driver. With increasing hump width the vertical acceleration of the driver increases, indicating greater discomfort.

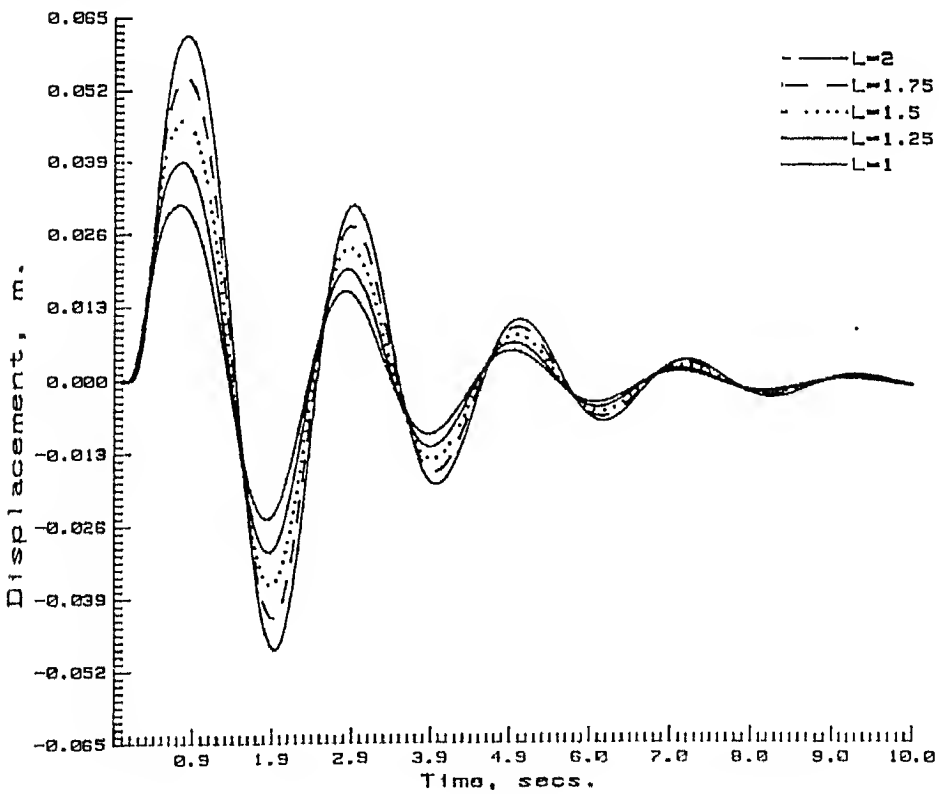

Fig. 16 Effect of varying the width of the hump on the displacement of driver. With increasing hump width vertical displacement of the driver increases.

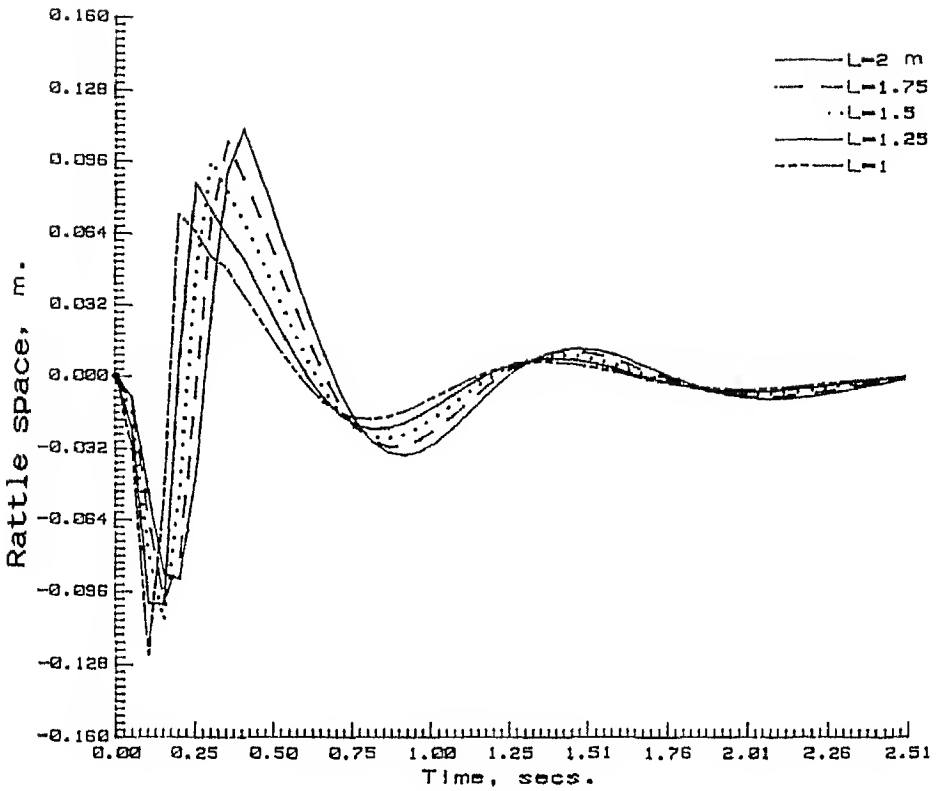

Fig. 17 Effect of varying the width of the hump on the rattle space at front end.

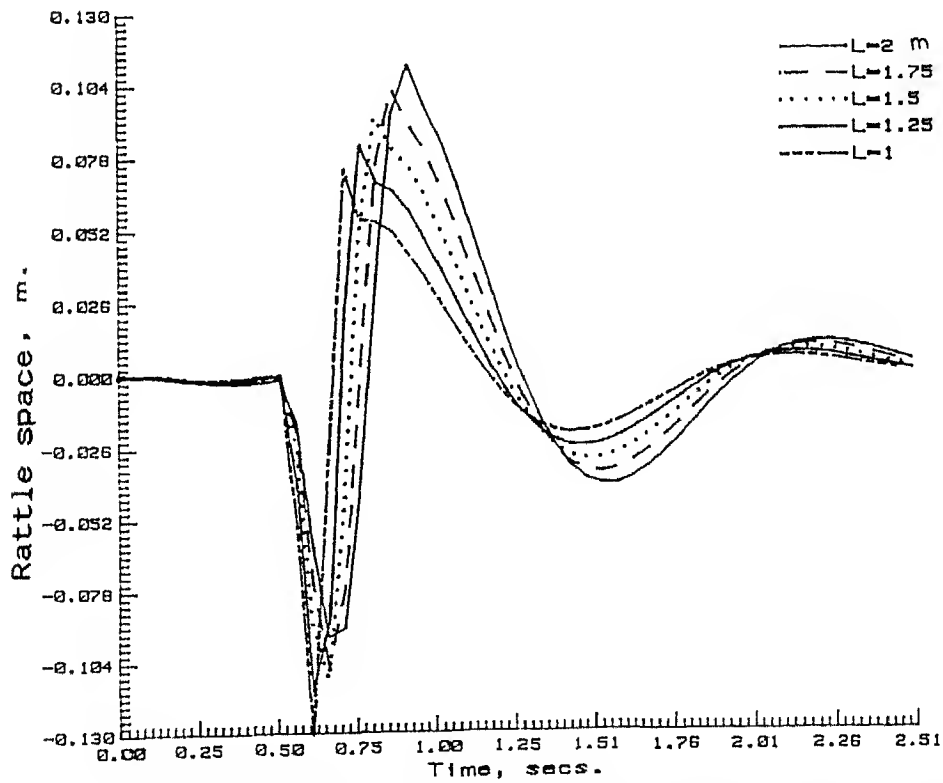

Fig. 18 Effect of varying the width of the hump on the rattle space at rear end. High rattle space indicates that the axle may touch the

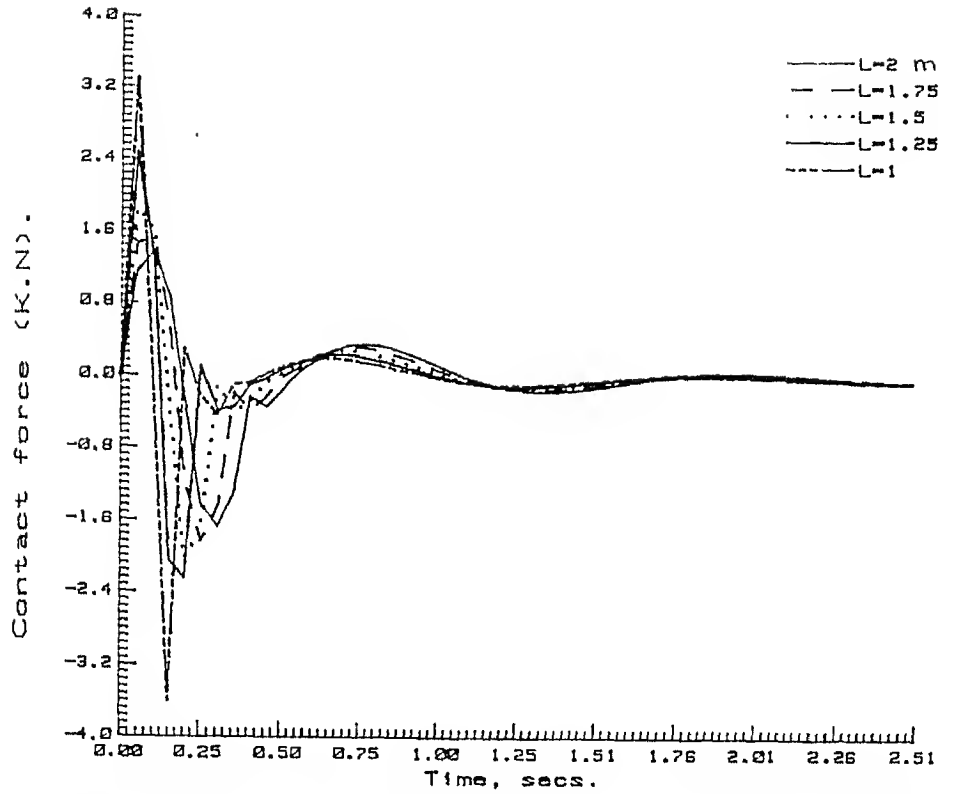

Fig. 19 Effect of varying the width of the hump on the wheel-road contact force at front end. Road contact force approaches to a constant value as hump width is increasing. These contact forces are deviations from the nominal contact force due to the weight of the vehicle.

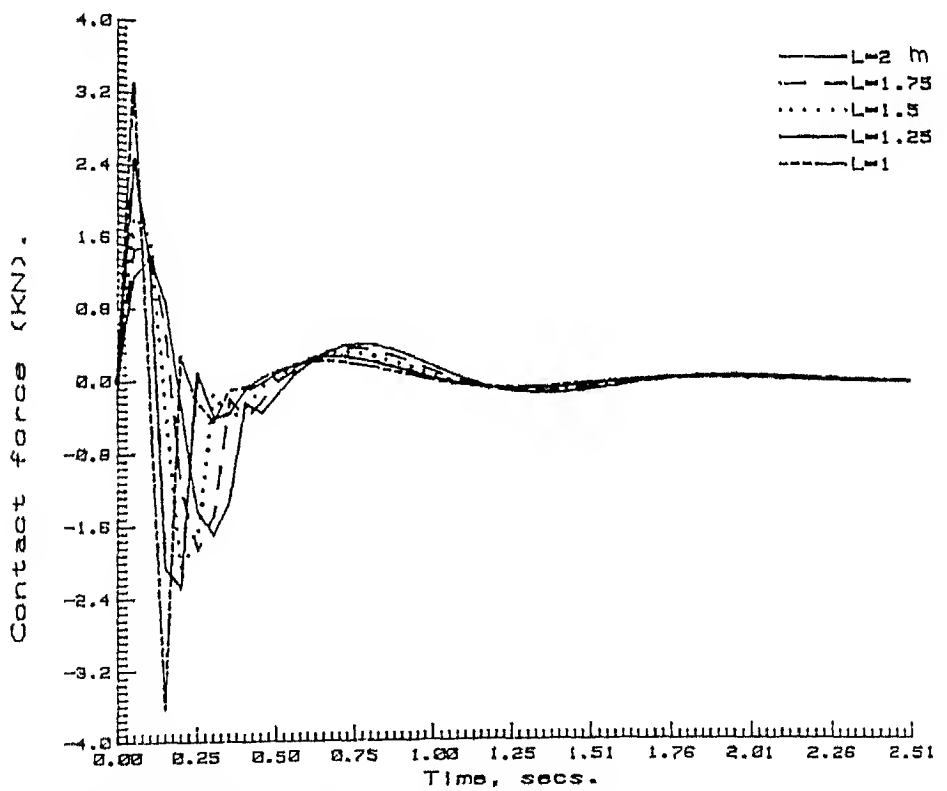

Fig. 20 Effect of varying the width of the hump on the wheel-road contact force at rear end.

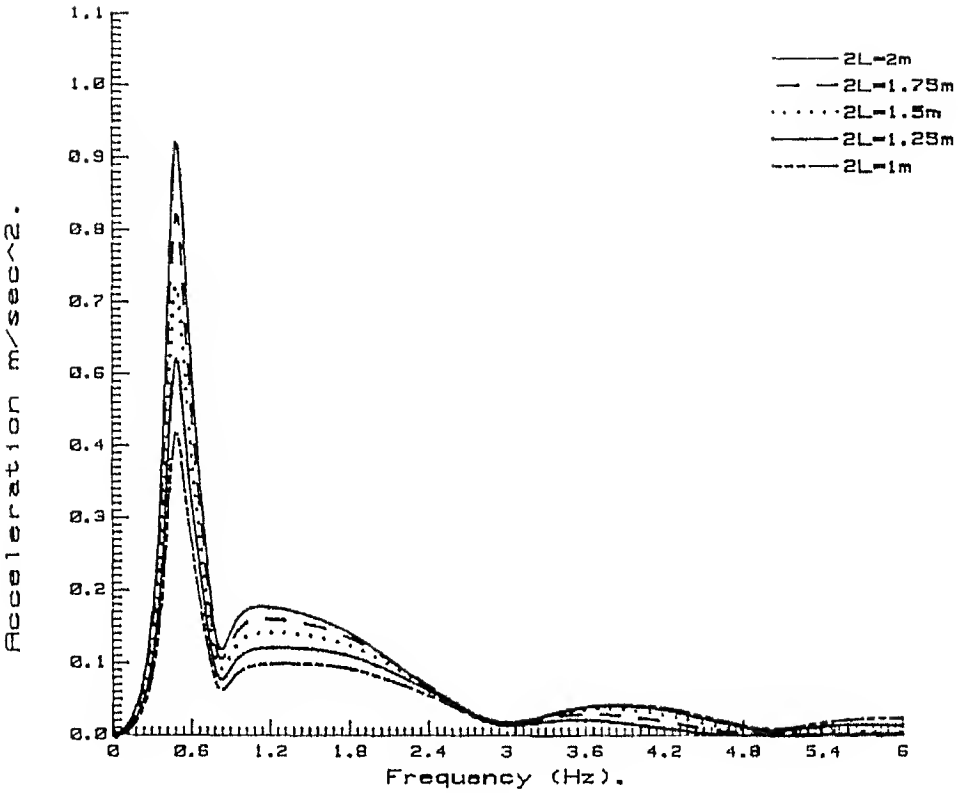

Fig. 21 Frequency response of driver's vertical acceleration for various hump widths. In general, at higher frequencies the same effects sre less bearable.

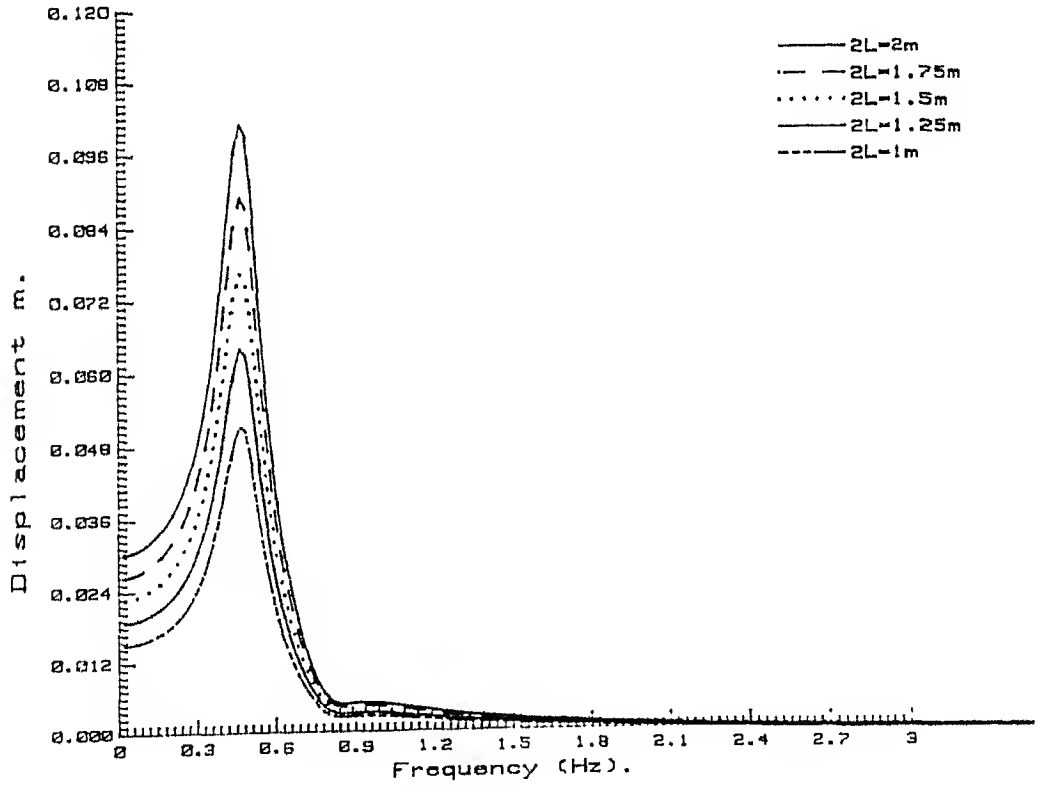

Fig. 22 Frequency response of driver's vertical displacement for various hump widths. According to sustained exposer studies, the comfort levels of human are non linearly reducing functions of frequencies. These do not apply to shock loads, but the general

The frequency domain magnitudes of vertical acceleration and displacement of driver (Fig. 21 and 22) also show an increasing effect with increase of hump width. This is because of the increasing crossing time with increasing width (i.e., the disturbance from road is acting for a longer time).

3.6 EFFECT OF VARYING HEIGHT OF THE HUMP

Five different maximum heights of humps are examined. These are 0.1, 0.15, 0.2, 0.25 and 0.3 m. Figures 23-29 show the effect of varying the hump height in time domain and figures 30 and 31 show this effect in frequency domain. As in the previous case the effect is very much the same.

3.7 EFFECT OF CROSSING SPEED

The significance of high speed is that the vehicle crosses the hump in shorter time. This can be noticed in all figures (32 - 38).Five different constant crossing speed are tried. They are 2, 3, 4, 5 and 6 m/sec. All aspects considered so far are having a tendency to decrease with increasing velocity except the road-tire contact force.

The tendency of increasing road-tire contact force is helpful in deciding whether a particular speed is allowable or not

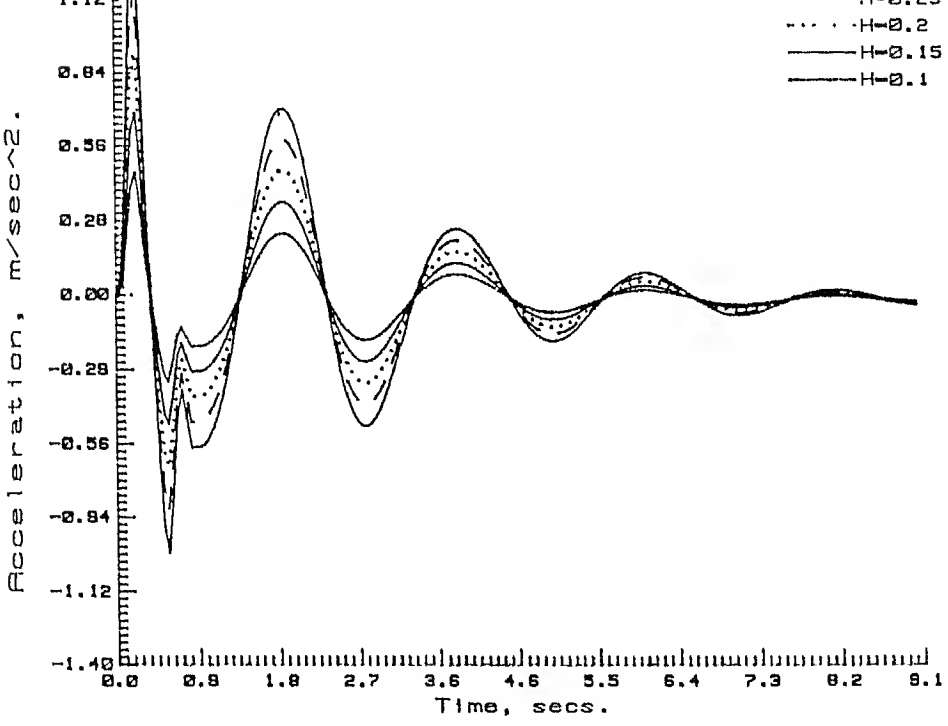

Fig. 23 Effect of varying the height of the hump on the acceleration of driver. Higher the hump height, higher will be the acceleration of the driver.

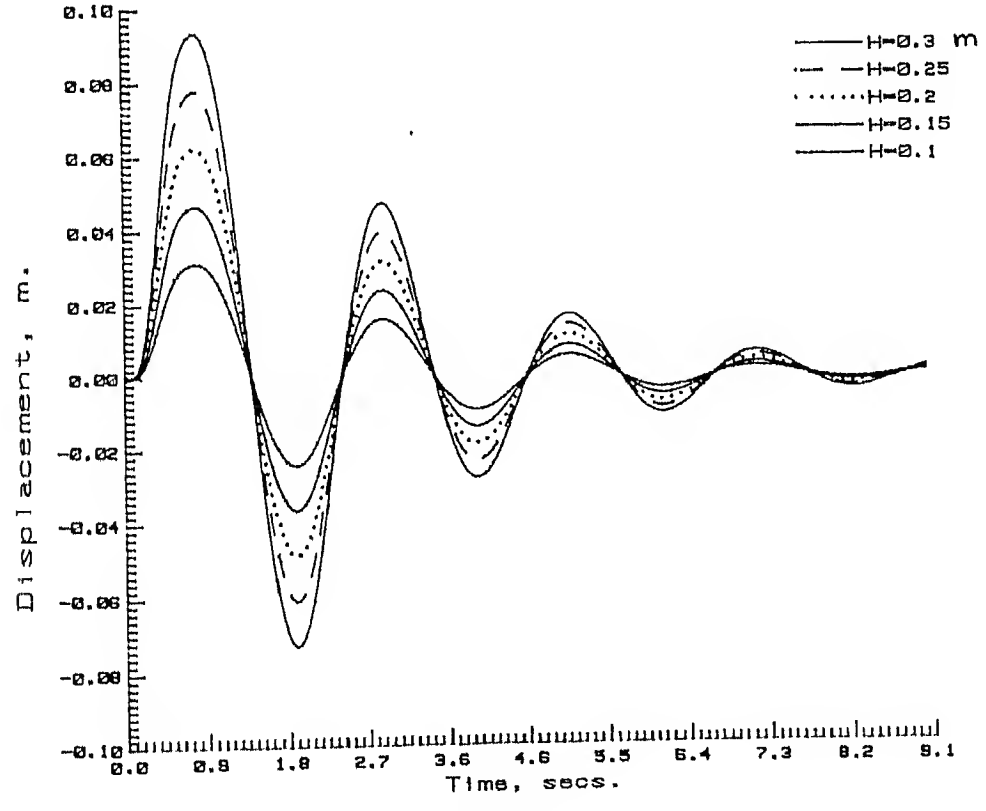

Fig. 24 Effect of varying the height of the hump on the displacement of driver.

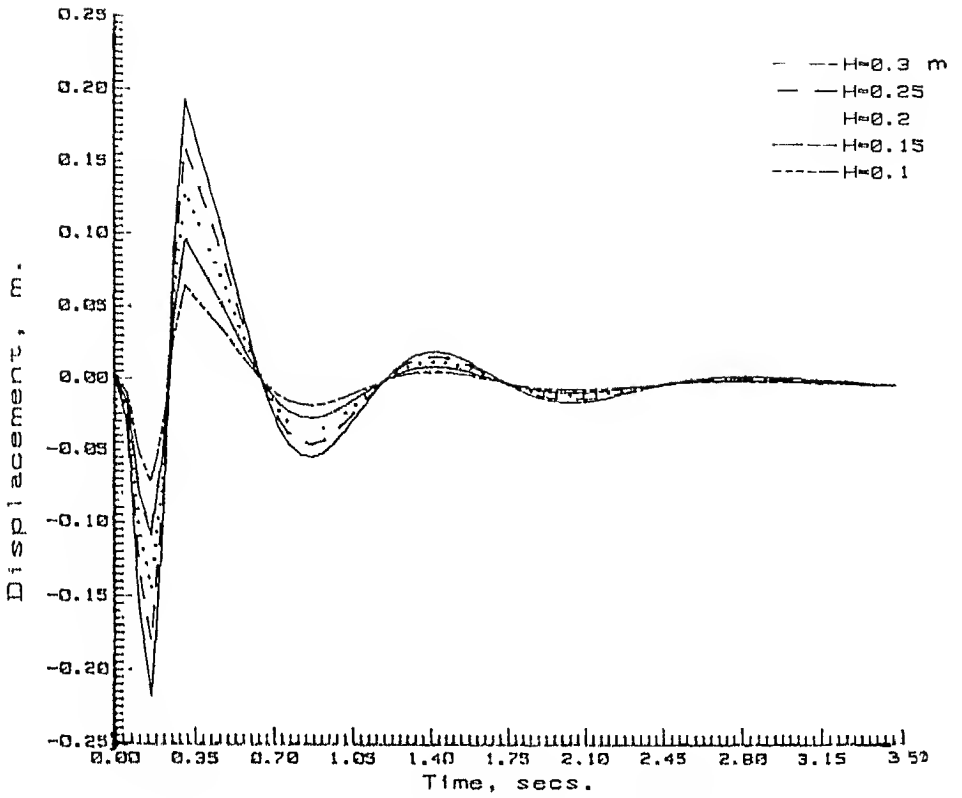

Fig. 25 Effect of varying the height of the hump on the rattle space at front end.

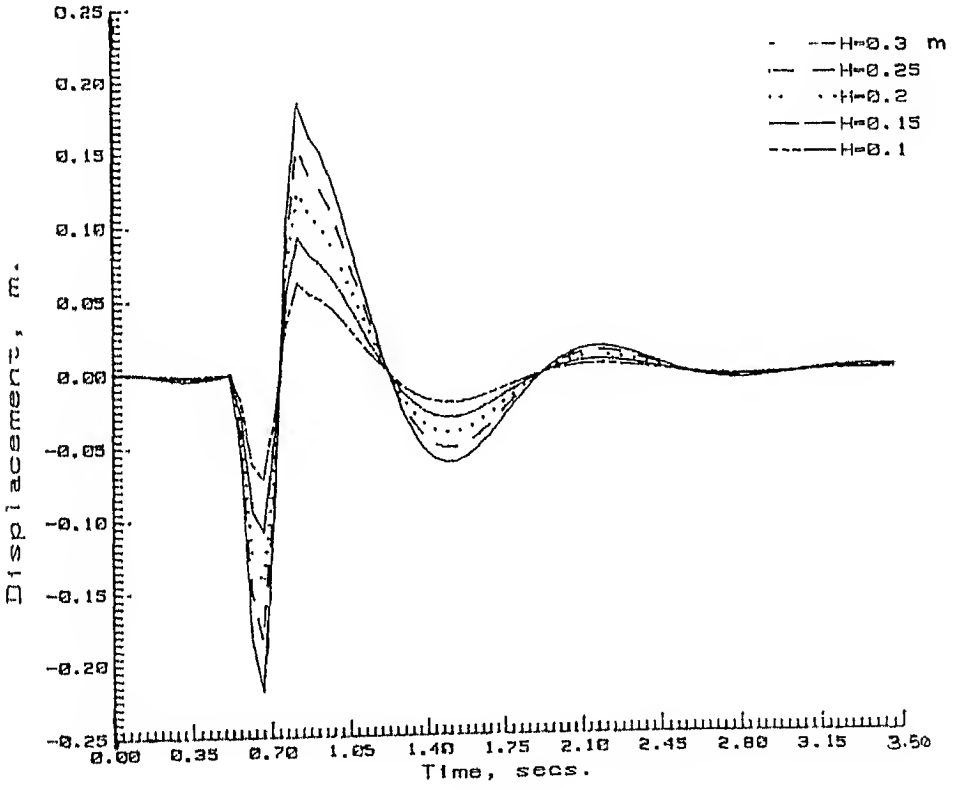

Fig. 26 Effect of varying the height of the hump on the rattle space at rear end.

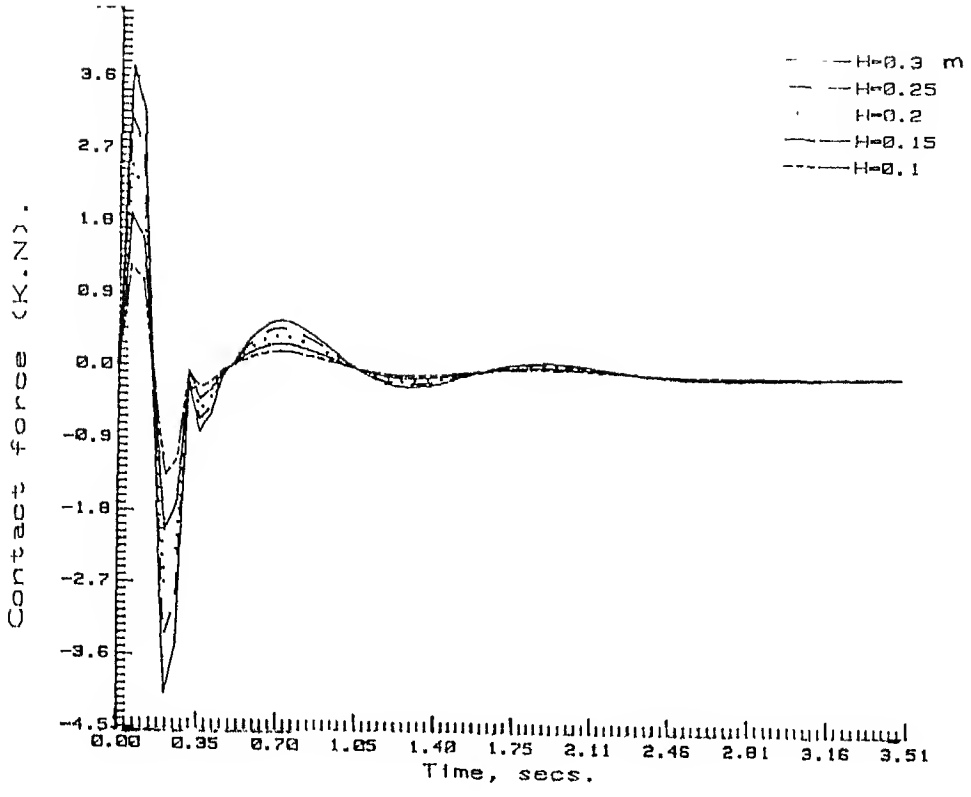

Fig. 27 Effect of varying the height of the hump on the wheel-road contact force at front end. These contact forces are deviations from nominal contact forces due to the weight of the vehicle.

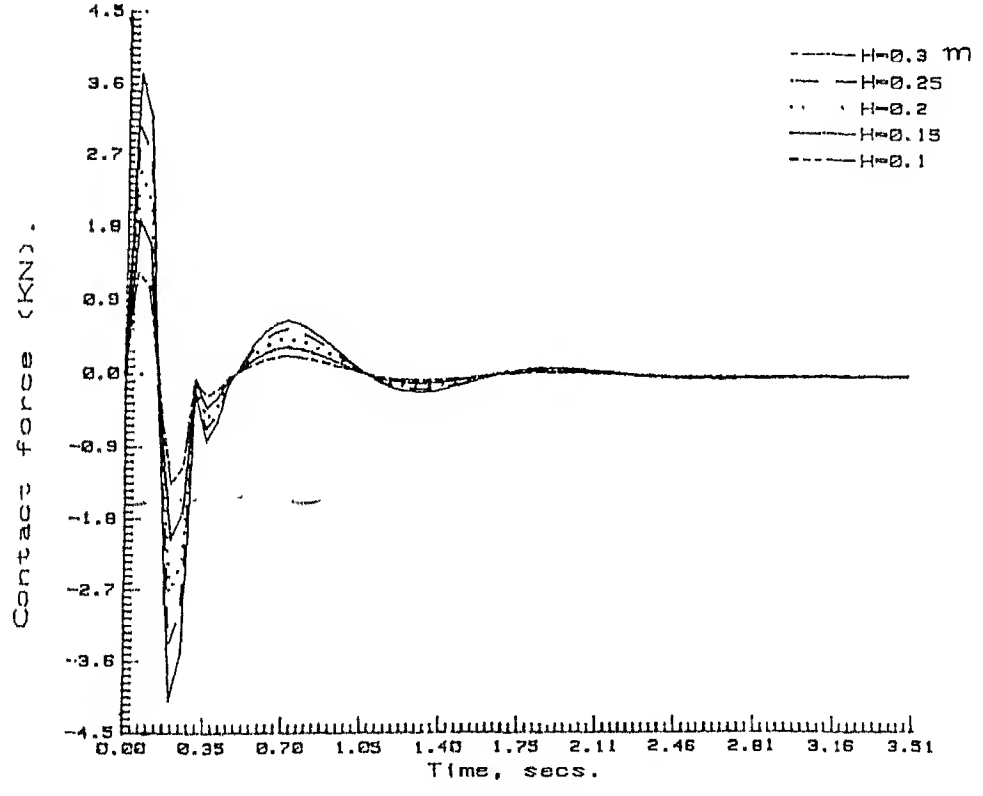

Fig. 28 Effect of varying the height of the hump on the wheel-road contact force at rear end.

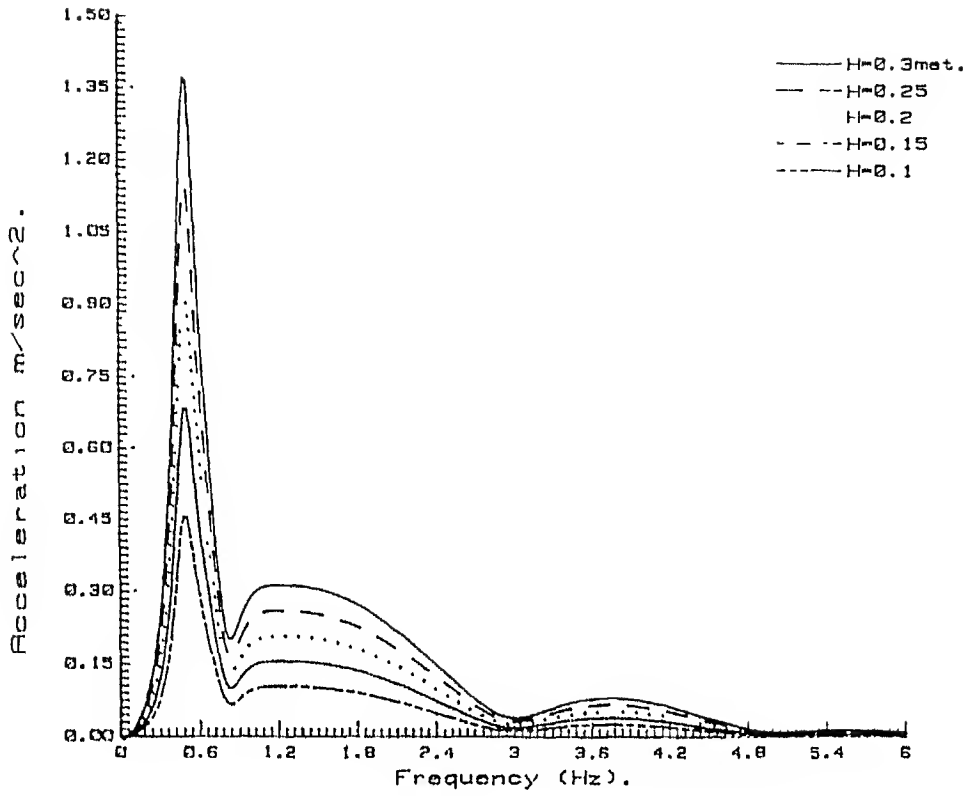

Fig. 29 Frequency response of driver's vertical acceleration for various hump heights.

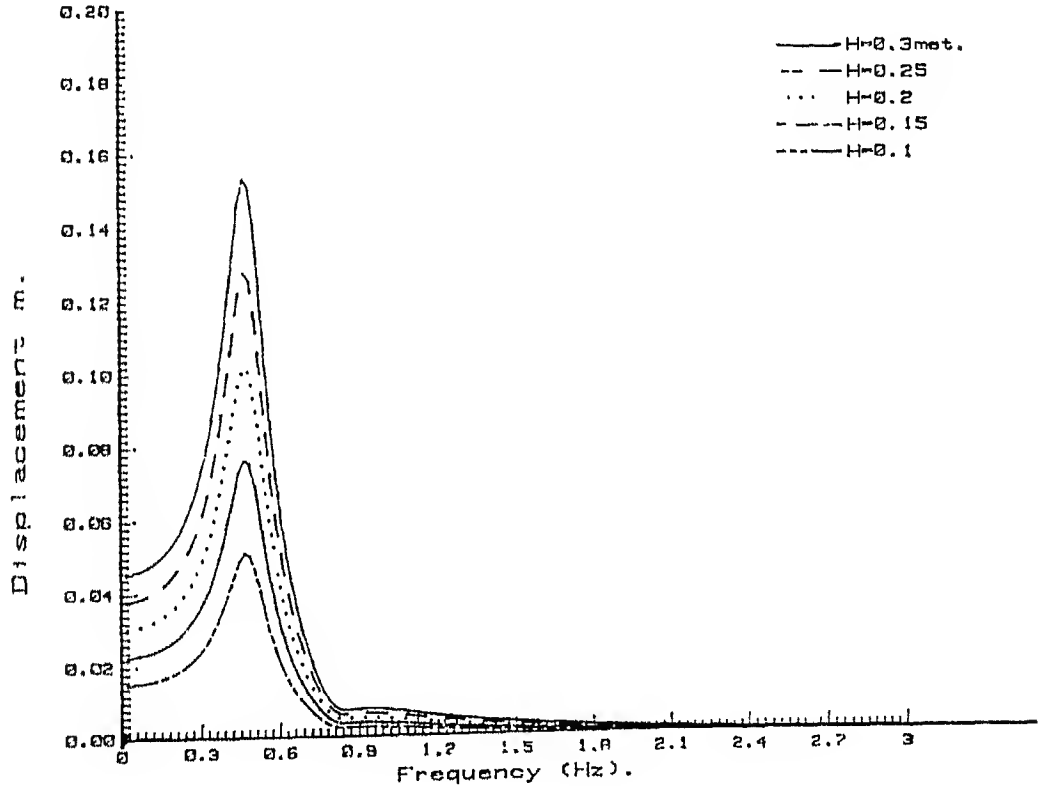

Fig. 30 Frequency response of driver's vertical displacement for various hump heights.

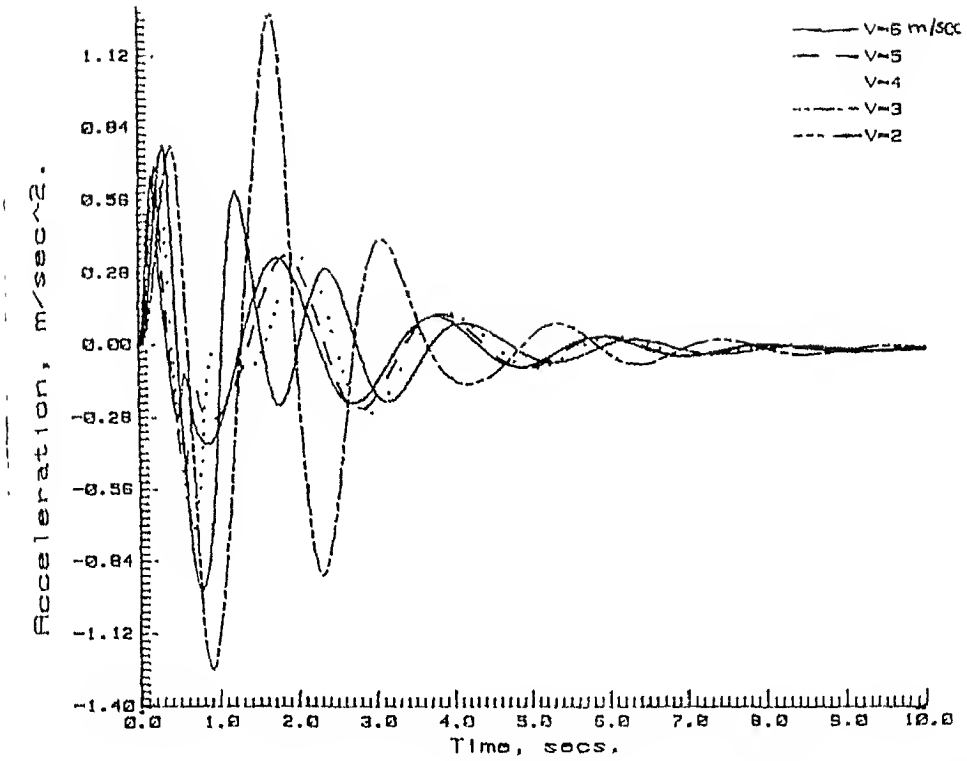

Fig. 31 Effect of crossing speed on the acceleration of driver. This result indicates that at speeds causing forcing frequencies greater than the natural frequency of the system, less energy is transferred to the system. Since permissible discomfort usually increases with acceleration, these results indicate greater comfort at higher speeds.

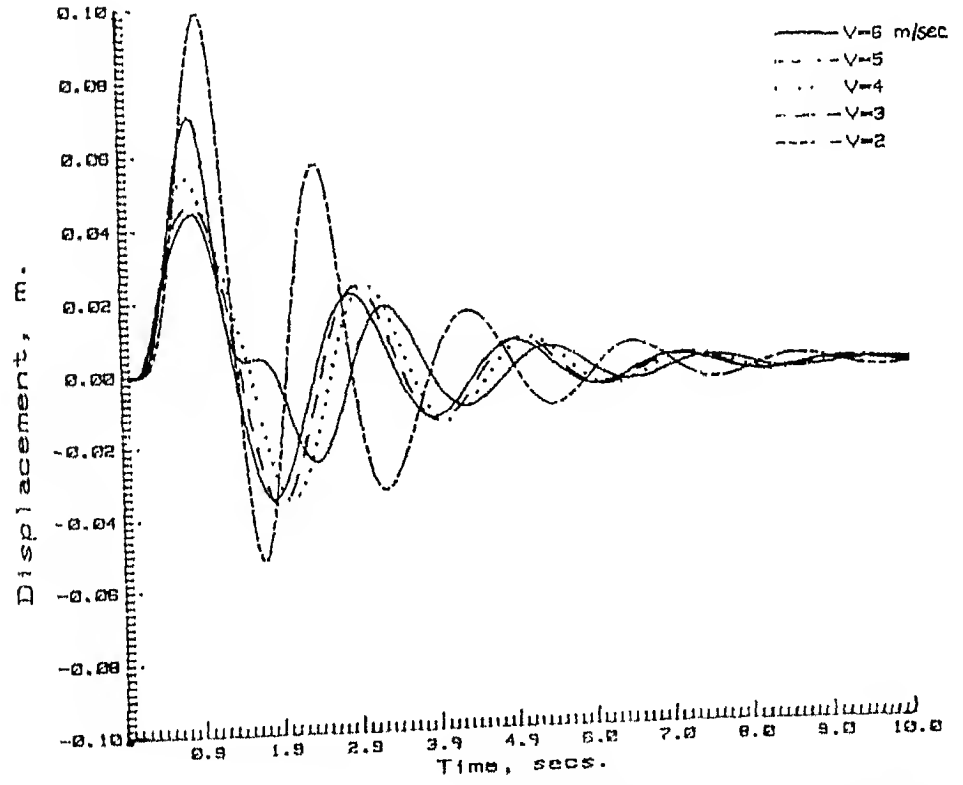

Fig. 32 Effect of varying the crossing speed on the displacement of

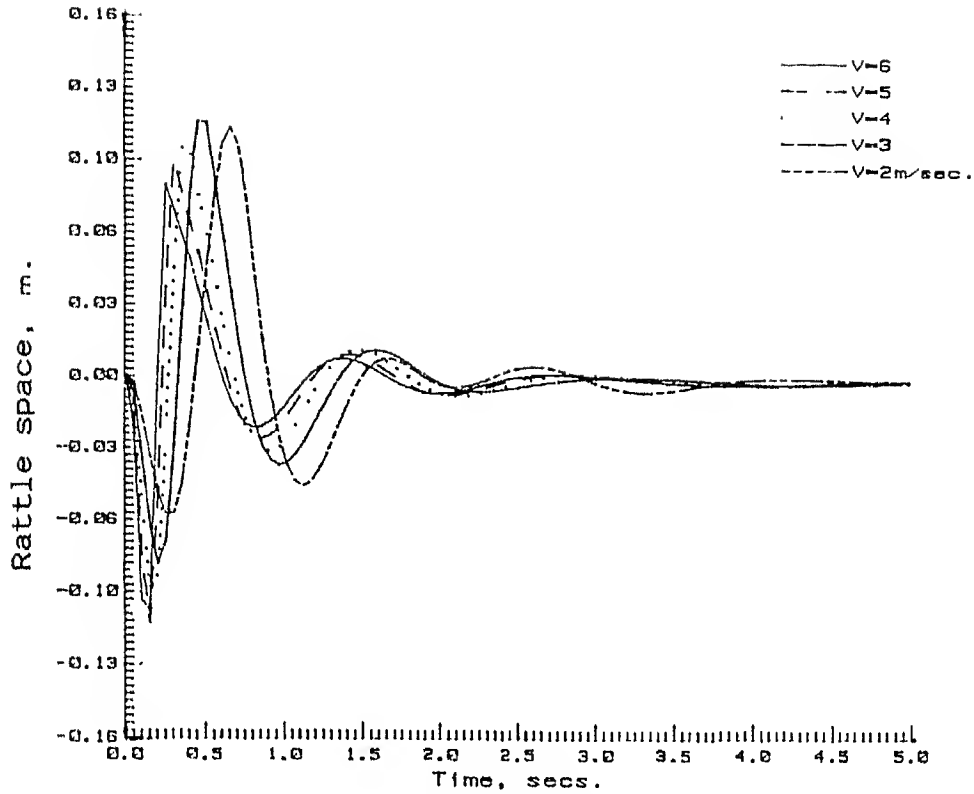

Fig. 33 Effect of varying the crossing speed on the rattle space at front end.

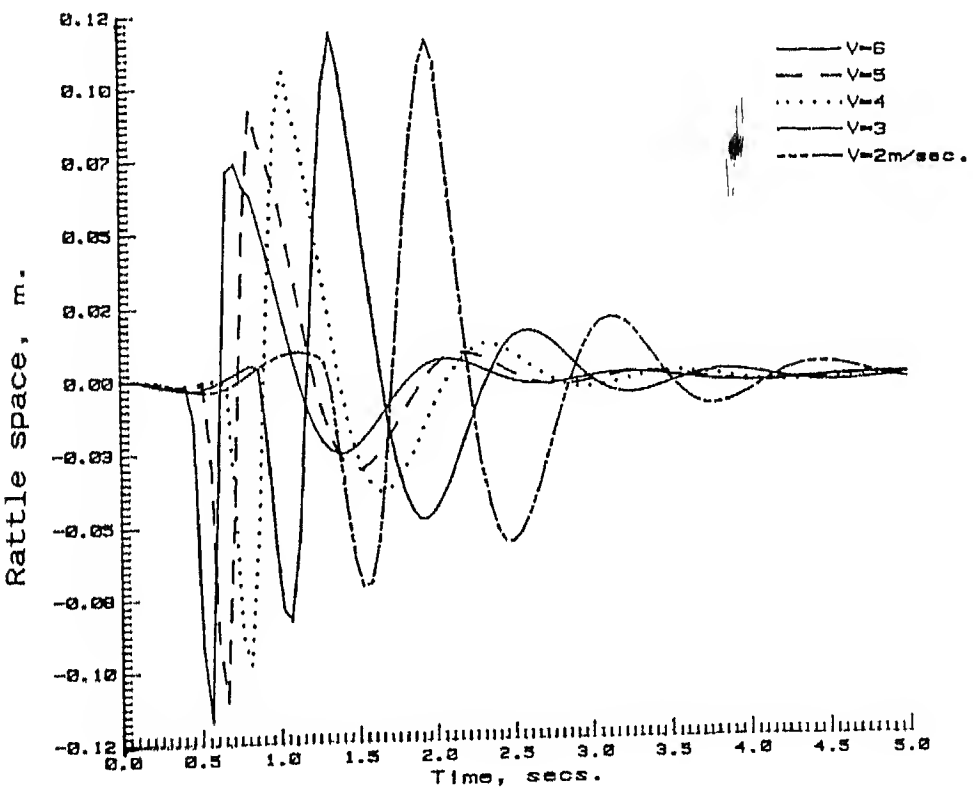

Fig. 34 Effect of varying the crossing speed on the rattle space at rear end.

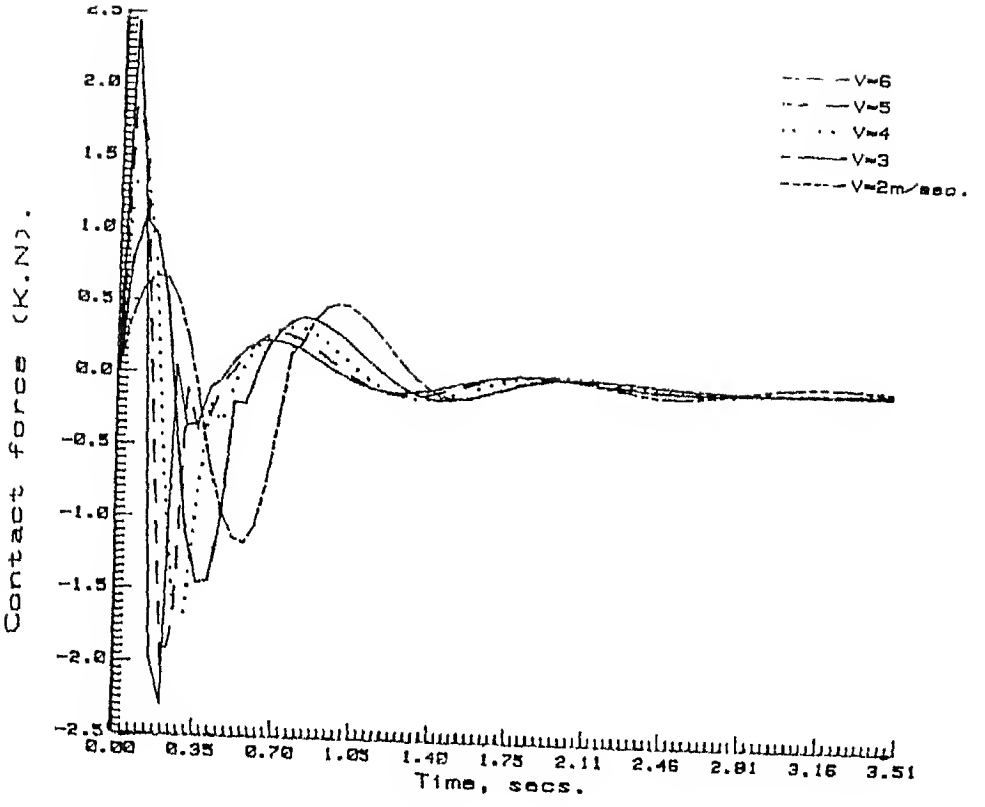

Fig. 35 Effect of varying the crossing speed on the wheel-road contact force at front end. These contact forces are deaviations from the nominal contact force due to the weight of the vehicle.

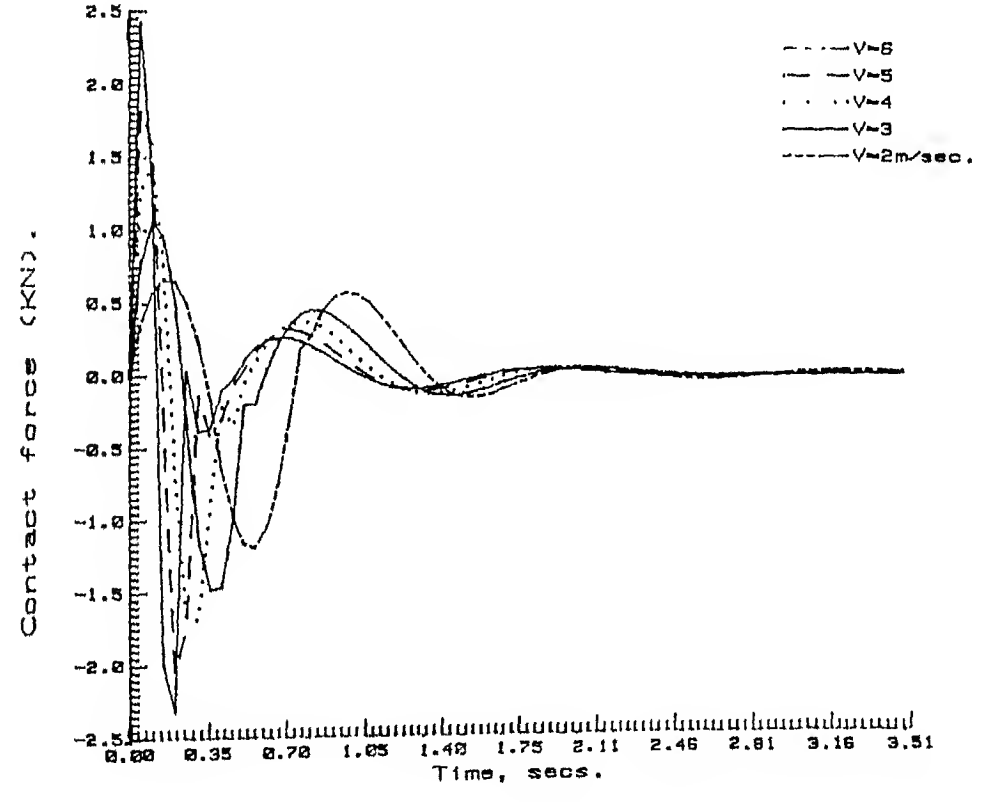

Fig. 36 Effect of varying the crossing speed on the wheel-road contact force at rear end.

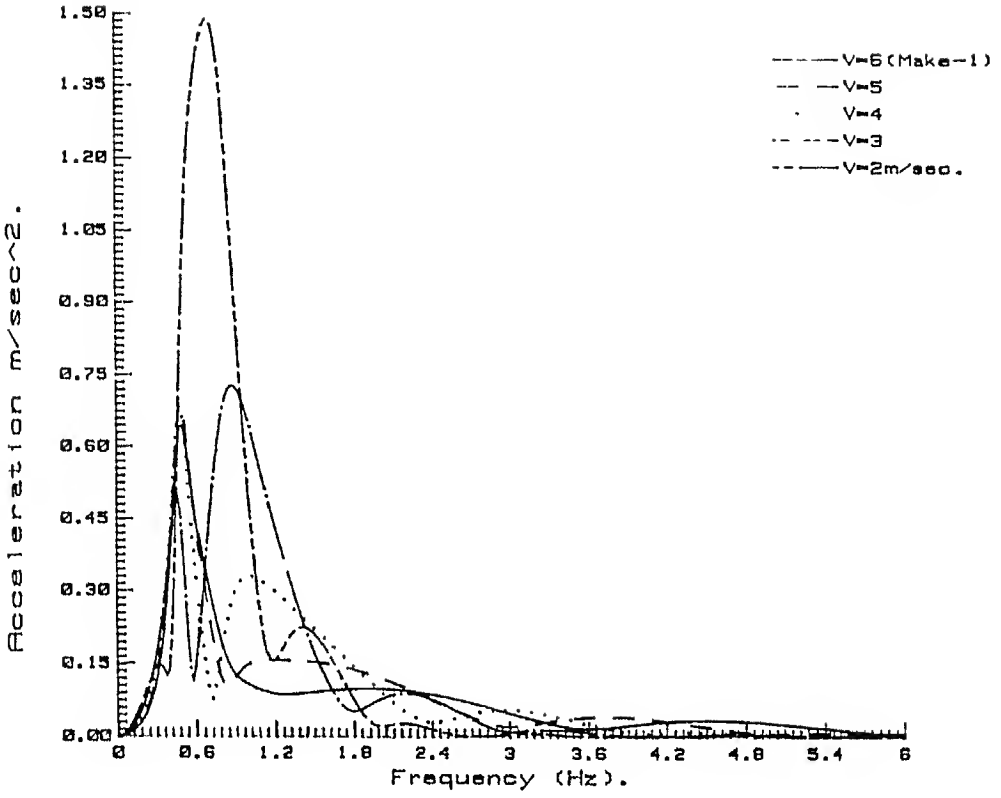

Fig. 37 Frequency response of driver's vertical acceleration for various crossing speeds.

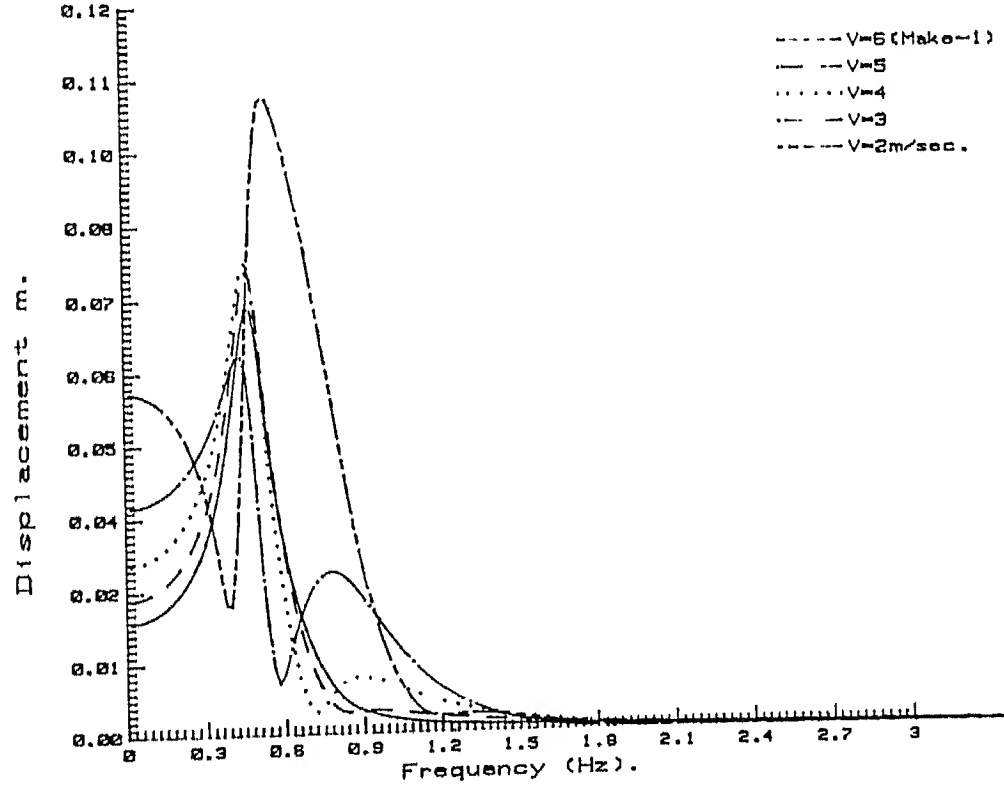

Fig. 38 Frequency response of driver's vertical displacement for various crossing speeds.

from safety point of view. It will be helpful to explain the decreasing effect of acceleration in frequency domain (Fig. 39). From this figure it is clear that for low velocities the magnitude of acceleration is dominant at low frequencies only. This can be tolerable because of low frequency. On the other hand, this magnitude is dominant at high frequency for high velocities, which is intolerable.

CHAPTER 4

CONCLUSIONS AND SCOPE FOR FURTHER WORK

We started the hump design process with the objective of: having little or no effect at low speeds and significant effect at high speeds. The following conclusions can be drawn based on the simulation results.

(1) The dynamic effect of humps vary considerably with the type of vehicle. The vehicles with large mass undergo comparatively greater dynamic effects.

(2) The hump parameters (height and width) also affect the dynamic response.

(3) For a given hump height (hump width) and crossing speed discomfort and suspension rattle space increases as hump width (hump height) increases.

(4) For a given hump height (hump width) and crossing speed, road contact force approaches a constant value as hump width (hump height) increases. This constant value is the same as that due to the stationary vehicle weight.

(5) Vertical acceleration of driver decreases as speed increases. Ride comfort is dependent on the vertical acceleration of the driver; the higher the acceleration, the less the ride comfort. Hence, ride comfort is likely to be better as speed increases.

The rms value of vertical acceleration increases with speed up to a maximum value (which depends on the vehicle type); as speed increases further the rms acceleration decreases. Intuitively this appears anomalous, but less energy is transferred to the vehicle as the frequencies increase well beyond the natural frequencies of the system. This is the inverse of the behavior a speed control device should have.

(6) Magnitude of road-holding force is directly proportional to the velocity of the vehicle. This is larger for vehicles with larger mass (Fig. 13).

(7) The magnitude of road holding force increases with speed up to a maximum value (which depend on the vehicle type) indicating good road holding; as speed increases further the magnitude of road holding force increases largely (thus increasing the hazards) while crossing a hump.

(8) Conclusions 4 and 6 further reveal that *in general the comfort increases and safety decreases with increasing crossing speed of the vehicle.*

(9) Given the limiting/allowable contact forces these simulation results give the fly-off velocity of vehicle for travel a cross ahump.

(10) Frequency dependency of driver's vertical acceleration and displacement are also presented for a class of humps. These can be directly used to test the acceptability of a hump if any test data in this field is available.

What do these results imply for hump design. Specifically it appears that rider comfort cannot be a factor in hump design, since comfort improves at high speeds. On the other hand, rattle space and road holding (i.e., safety) decreases as speed increases.

These results appear to be contrary to normal intuition, and experience while travelling over humps. A possible explanation to these contrary results evolved after the work was finished. The reasons can be explained with reference to a 1-DOF vehicle model (Fig. 2). The following figure shows the frequency domain input for two different crossing speeds of the vehicle and the transfer function. Typically, at higher velocity, frequency domain input has a wider frequency spread, but lesser amplitudes.

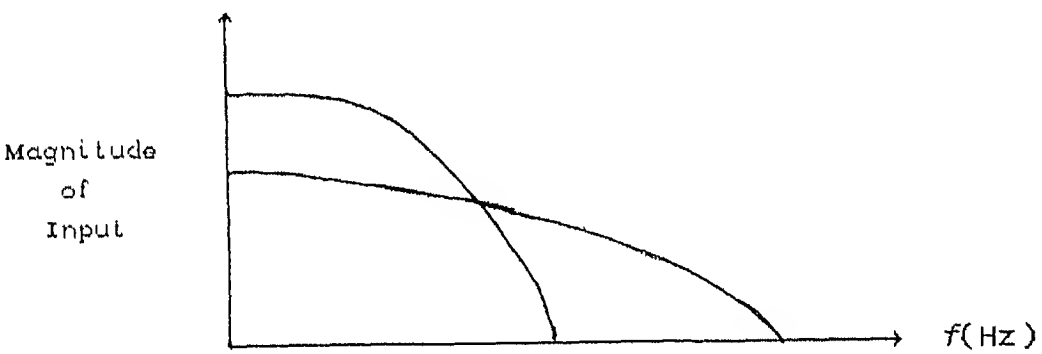

Figure showing the frequency domain input for two different crossing speeds of the vehicle.

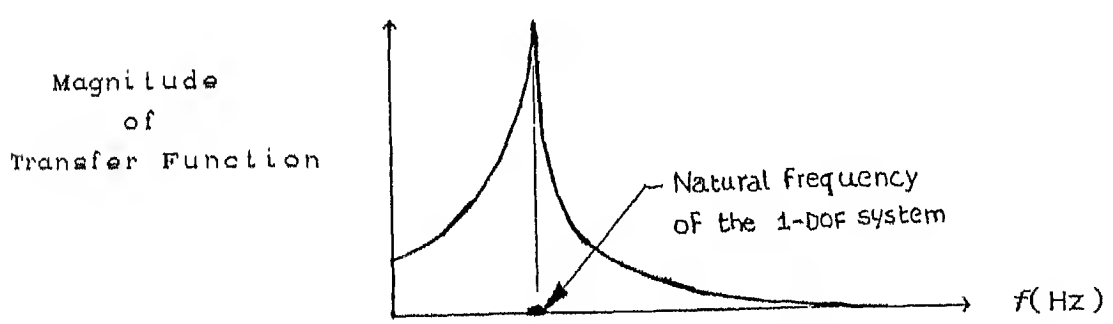

Figure showing transfer function for 1-DOF vehicle model.

It can be seen from these figures, the input (hump) is such that at velocities V_1 and V_2, both are present even after the natural frequency of the system, except that their magnitudes are different. The vehicle while travelling the at a lesser speed (V_1) absorbs more

energy compared to travel at a higher velocity velocity (V_2) since the amplitude of frequency domain input is higher. This could be the reason why the results are contrary to intuition.

On the other hand if we choose a hump profile whose frequency domain input for two different velocities appears like the one shown in the below figure, then it would be possible to achieve the objective of design of a hump.

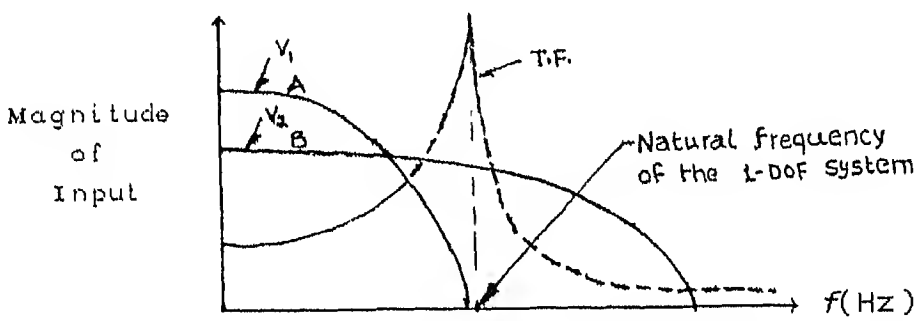

Figure showing the frequency domain input for two different crossing speeds of the vehicle.

Further work needs to try to choose humps such that at low speeds the forcing input appears as the input A and at higher velocity as the input B. In this type of hump profile the true objective of hump design may be achieved.

Another correction that would be desirable in future work could be to prevent the total contact force from becoming negative. This would imply that the tire can be pulled down by the ground which is impossible. To correct for this, the forcing function should be nonlinear in the sense that the function cannot go below zero. However this would lead to considerable complexity of since one would then need to model the effect of impact after loosing contact.

APPENDIX A

STATE-SPACE EQUATION

From the car body, front and rear suspensions, tires and seat, the state-space equation of the vehicle modal in matrix form is:

$$\dot{X}(t) = A.X(t) + B.U(t)$$

The 16-components of state variable vector is:

$$X = [\, x_o,\ x_1,\ x_2,\ x_3,\ x_4,\ x_5,\ \psi,\ \phi,\ \dot{x}_o,\ \dot{x}_1,\ \dot{x}_2,\ \dot{x}_3,\ \dot{x}_4,\ \dot{x}_5,\ \dot{\psi},\ \dot{\phi}\,]^T$$

The input vector is:

$$U = [\, w_1,\ \dot{w}_1,\ w_2,\ \dot{w}_2,\ w_3,\ \dot{w}_3,\ w_4,\ \dot{w}_4,\ 0,\ cf,\ \rho,\ 0\,]^T$$

where cf is the force due to centrifugal effect and is equal to $(m_s.V^2R/h)$ and ρ is the force that arises due to acceleration and deceleration effects and is equal to $(m_s.a.h)$. Here R is the reciprocal of curvature of turning circle of the vehicle, h is the height of the center of mass of the vehicle sprung mass, and a is the acceleration or deceleration(m/sec^2) of the vehicle. Here uniform velocity is assumed ($cf = \rho = 0$).

The state equation matrices can be expressed from (12) and (13) as:

$$A = \begin{bmatrix} 0_{8\times8} & I_{8\times8} \\ [-M^{-1}.K]_{8\times8} & [-M^{-1}.C]_{8\times8} \end{bmatrix}_{16\times16,} \qquad B = \begin{bmatrix} B_{11} \\ B_{22} \end{bmatrix}_{16\times8}$$

where,

$$B_{11} = [0]_{8\times8} \qquad B_{22} = \begin{bmatrix} b_1 & b_2 & 0 & 0 & 0 & 0 & 0 & 0 \\ 0 & 0 & b_3 & b_4 & 0 & 0 & 0 & 0 \\ 0 & 0 & 0 & 0 & b_5 & b_6 & 0 & 0 \\ 0 & 0 & 0 & 0 & 0 & 0 & b_7 & b_8 \\ 0 & 0 & 0 & 0 & 0 & 0 & 0 & 0 \\ 0 & 0 & 0 & 0 & 0 & 0 & 0 & 0 \\ 0 & 0 & 0 & 0 & 0 & 0 & 0 & 0 \\ 0 & 0 & 0 & 0 & 0 & 0 & 0 & 0 \end{bmatrix}_{8\times8}$$

Matrix M: It is a diagonal mass matrix with elements:

$m_{11} = m_1$, $m_{22} = m_2$, $m_{33} = m_3$, $m_{44} = m_4$,

$m_{55} = m_5$, $m_{66} = I_r$, $m_{77} = I_p$, $m_{88} = m_o$.

Matrix K: It is a symmetric matrix with spring constants and its elements are as follows:

$k_{1,1} = -(k_{11} + k_{21})$, $k_{1,5} = k_{11}$, $k_{1,6} = -S.k_{11}$, $k_{1,7} = k_{11}.l_1$

$k_{2,2} = -(k_{12} + k_{22})$, $k_{2,5} = k_{12}$, $k_{2,6} = S.k_{12}$, $k_{2,7} = k_{12}.l_1$

$k_{3,3} = -(k_{13} + k_{23})$, $k_{3,5} = k_{13}$, $k_{3,6} = -S.k_{13}$, $k_{3,7} = -k_{13}.l_2$

$k_{4,4} = -(k_{14} + k_{24})$, $k_{4,5} = k_{14}$, $k_{4,6} = S.k_{14}$, $k_{4,7} = -k_{14}.l_2$

$k_{5,5} = -(k_{11} + k_{12} + k_{13} + k_{14} + k_o)$

$k_{5,6} = S.(k_{11} - k_{12} + k_{13} - k_{14}) + l_x.k_o$

$k_{5,7} = -l_1.(k_{11} + k_{12}) + l_2.(k_{13} + k_{14}) - k_o.l_y$

$k_{5,8} = k_o$

$k_{6,6} = -S^2(k_{11} + k_{12} + k_{13} + k_{14}) - l_x^2.k_o$

$k_{6,7} = -S.l_1.(k_{12} - k_{11}) - S.l_2.(k_{13} - k_{14}) + l_x.l_y.k_o$

$k_{6,8} = -l_x.k_o$

$k_{7,7} = -l_1^2.(k_{11}+k_{12}) - l_2^2.(k_{13}+k_{14}) - l_y^2.k_o$

$k_{7,8} = l_y.k_o$

$k_{8,8} = -k_o$

Matrix C: It is a symmetric matrix with damper coefficients and its elements are as follows:

$C_{1,1} = -(C_{11} + C_{21})$, $C_{1,5} = C_{11}$, $C_{1,6} = -S.C_{11}$, $C_{1,7} = C_{11}.l_1$

$C_{2,2} = -(C_{12} + C_{22})$, $C_{2,5} = C_{12}$, $C_{2,6} = S.C_{12}$, $C_{2,7} = C_{12}.l_1$

$C_{3,3} = -(C_{13} + C_{23})$, $C_{3,5} = C_{13}$, $C_{3,6} = -S.C_{13}$, $C_{3,7} = -C_{13}.l_2$

$C_{4,4} = -(C_{14} + C_{24})$, $C_{4,5} = C_{14}$, $C_{4,6} = S.C_{14}$, $C_{4,7} = -C_{14}.l_2$

$C_{5,5} = -(C_{11} + C_{12} + C_{13} + C_{14} + C_o)$

$C_{5,6} = S.(C_{11} - C_{12} + C_{13} - C_{14}) + l_x.C_o$

$C_{5,7} = -l_1.(C_{11} + C_{12}) + l_2.(C_{13} + C_{14}) - C_o.l_y$

$C_{5,8} = C_o$

$C_{6,6} = -S^2.(C_{11} + C_{12} + C_{13} + C_{14}) - l_x^2.C_o$

$C_{6,7} = -S.l_1.(C_{12} - C_{11}) - S.l_2.(C_{13} - C_{14}) + l_x.l_y.C_o$

$C_{6,8} = -l_x.C_o$

$C_{7,7} = -l_1^2.(C_{11}+C_{12}) - l_2^2.(C_{13}+C_{14}) - l_y^2.C_o$

$C_{7,8} = l_y.C_o$

$C_{8,8} = -C_o$

NOTE: In the above matrices elements specified other than symmetric elements are all zeros.

APPENDIX B

Data for two vehicle models (Make-1 and Make-2) used in the present work are given in the below Table.

Parameter	*Symbol*	*Units*	*Make-1*	*Make-2*
Car body mass	m_5	Kg	1 090	2 000
Car body mass moment of Inertias:				
In Pitching	I_p	Kg-m^2	1 680	3 200
In Rolling	I_r	Kg-m^2	250	510
Front unsprung mass	m_1, m_2	Kg	27.5	25.0
Rear unsprung mass	m_3, m_4	Kg	25.0	25.0
Suspension stiffness:		N/m		
Front	k_{11}, k_{12}		7 500	20 000
Rear	k_{21}, k_{22}		7 500	20 000
Suspension damping:		N.s/m		
Front	C_{11}, C_{12}		1 000	1 500
Rear	C_{21}, C_{22}		1 000	1 500
Tire stiffness		N/m		
Front	k_{21}, k_{22}		75 000	90 000
Rear	k_{23}, k_{24}		75 000	90 000
Tire damping		N.s/m		
Front	C_{21}, C_{22}		200	275
Rear	C_{23}, C_{24}		200	275
Wheel-base	W	m	2.5	2.5
Wheel-track	S	m	0.7	0.7
Front length	l_1	m	1.4	1.3
Rear length	l_2	m	1.1	1.2
Seat total mass	m_o	Kg	100	100
Seat spring stiffness	k_o	N/m	1 500	10 000
Seat damping coeff.	C_o	N.s/m	150	500
Seat X-position	l_x	m	0.4	0.5
Seat Y-position	l_y	m	0.35	0.35

REFERENCES

1 Antonio Moran., and Masao Nagai., "Analysis and Design of Active Suspensions by $H\infty$ Robust Control Theory," JSME *International Journal*, Series III, 1993, Vol. 35, No. 3, pp. 427-437.

2 Dahlberg, T., "Parametric Optimization of a 1-DOF vehicle travelling on a Randomly profiled Road," *Journal of Sound and Vibration*, (1977), 55, pp. 245-253.

3 Dahlberg, T., "Ride comfort and Road holding of A 2-DOF vehicle Travelling on a Randomly Profiled Road," *Journal of Sound and Vibration* (1978), 58(2), pp. 179-187.

4 Del Castillo, J.M., Pintado, P. and Benitez. F.A., "Optimization For Vehicle Suspension II: Frequency Domain," *Vehicle System Dynamics*, 19(1990), pp. 331-352.

5 Demic, M., "A Contribution to the Optimization of the Characteristics of Elasto Damping Elements of Passenger Cars," *Vehicle System Dynamics*, 19(1990), pp. 3-18.

6 Essam Kassem., and Yaagoub Al-Nassar, "Dynamic Consideration of Speed Control Humps," *Transpn Res - B*, Vol. 16B, No. 4, pp. 291-302.

7 Hrovat, D., "Applications of Optimal Control to Advanced Automobile Suspension Design," ASME *Journal of Dynamic Systems, Measurement, and Control*, June 1993, Vol. 115, pp. 328-342.

8 Meirovitch, L., *Analytical Methods in Vibrations*, Macmillan, New York, 1967.

9 Mohammed M. Elmadany., "Ride Performance Potential of Active Fast Load Leveling Systems," *Vehicle System Dynamics*, 19(1990), pp. 19-47.

10 Nathoo, N.S., and Healey, A.J., "Coupled Vertical-Lateral Dynamics of a Pneumatic Tired Vehicle: Part I – A mathematical Model," ASME *Journal of Dynamic Systems, Measurements and Control*, December 1978, Vol. 100, pp. 311-318.

11 Nathoo, N.S., and Healey, A.J., "Coupled Vertical-Lateral Dynamics of a Pneumatic Tired Vehicle: Part II – Simulated Versus Experimental Data," ASME *Journal of Dynamic Systems, Measurements and Control*, December 1978, Vol. 100, pp. 319-325.

12 Newland, D.E., *Mechanical Vibration Analysis and Computation*, Longman, London, 1989.

13 Pintado, P., and Benitez, F.G., "Optimization For Vehicle Suspension I: Time Domain," *Vehicle System Dynamics*, 19(1990), pp. 273-288.

14 Smith, C.C., Mc Gehee, D.Y., and Healey, A.J., "The prediction of Passenger Ride Comfort From Acceleration Data," ASME *Journal of Dynamic Systems, Measurements, and Control*, March 1978, Vol. 100, pp. 34-41.

15 Smith, C.C., Kwak, Y.K., "Identification of the Dynamic Characteristics of Bench-Type Automotive Seat for the Evaluation of the Ride Quality," ASME *Journal of Dynamic Systems, Measurements, and Control*, March 1978, Vol. 100, pp. 42-49.

16 Thompson, A.G., and Davis, B.R., "Optimal Active Suspension Design Using a Frequency-shaping PID filter," *Vehicle System Dynamics*, 21(1992), pp. 19-37.

17 Thompson, W.T., *Theory of Vibrations With Applications* (3rd edition), CBS, 1988.

ME-1994-M-GCP-DES